NOTES ON CRYSTALLOGRAPHY

They have been written to provide the students of Earth Sciences/Materials Sciences with a support to lessons in classroom, and handed out accordingly. Note that:

- **they do not represent a ‘’textbook’’, but a bare integration, not-exhaustive, of what is discussed in classroom;**
- **mistakes are present, as the presently available version is still on development;**
- **many pictures have been downloaded from the internet. Parts of the present text about detectors are from the internet.**

OUTLINE

I. SOME CONCEPTS ABOUT THE NOTION OF ‘’CRYSTAL STRUCTURE’’

Crystal: a solid state phase, whose atoms are arranged according to a fully defined order characterised by *translational invariance*. A crystal can be generated by *lattice-translating* its elementary cell’s content. Because of the ordered atomic distribution, crystals exhibit anisotropic properties, *i.e*. features depending on the direction. A perfectly disordered system, *i.e*. amorphous, shows isotropic properties, *i.e*. features independent of direction. Let us look at a crystal as an array of equal ‘’*bricks*’’ set adjacent to each other; they schematically correspond to the elementary cells.

Elementary cell: the volume of a crystal (*i.e*. a ‘’fragment’’) containing a set of atoms sufficient to reproduce the full structure by lattice translations. The smallest elementary cell is called *primitive cell*. The elementary cell is defined by three vectors (**a**,**b**,**c**), which define its edges and are called *basic lattice vectors*.

Lattice translation: any vector defined as

$$n\,\mathbf{a} + m\,\mathbf{b} + p\,\mathbf{c} \qquad \text{(I.1)}$$

where *n*, *m*, *p* are integer numbers (0,±1, ±2,..). The set of all the lattice translations is usually called ‘’*lattice*’’.

Generating a crystal: let us assume to have an elementary cell, *i.e* a finite volume delimited by (**a**,**b**,**c**), and containing atoms. The full crystal structure can be generated by “projecting” in the space every point **x** of the elementary cell’s volume using all the possible lattice translations, *i.e.*

$$\mathbf{x} \rightarrow \mathbf{x} + n\,\mathbf{a} + m\,\mathbf{b} + p\,\mathbf{c} \qquad \text{(I.2)}$$

Translational invariance: given two points of a crystal, $\mathbf{x}_1$ and $\mathbf{x}_2$, if they are such that $\mathbf{x}_1-\mathbf{x}_2=\mathbf{T}$, where **T** is a lattice translation vector, then the properties at $\mathbf{x}_1$ are equal to those at $\mathbf{x}_2$. This is equivalent to say that if $\rho(\mathbf{x})$ fixes a generic property of the crystal at **x** (electron density, electric field component, etc..), then

$\rho(\mathbf{x}) = \rho(\mathbf{x}+\mathbf{T}) \quad \forall\ \mathbf{T}$, where $\mathbf{T} = n\,\mathbf{a} + m\,\mathbf{b} + p\,\mathbf{c}$.

In other words, any function describing properties of a crystal exhibits a *periodicity* according to the lattice of the crystal.

Crystal structure: ordered atomic arrangement constituting a crystal. The crystal structure is obviously invariant upon any *lattice translation*. The figure beneath displays a case of 2D-crystal structure, here used for the sake of simplicity. Note the elementary cell edges, marked by black lines, and basic lattice vectors (**a**,**b**), displayed by arrows.

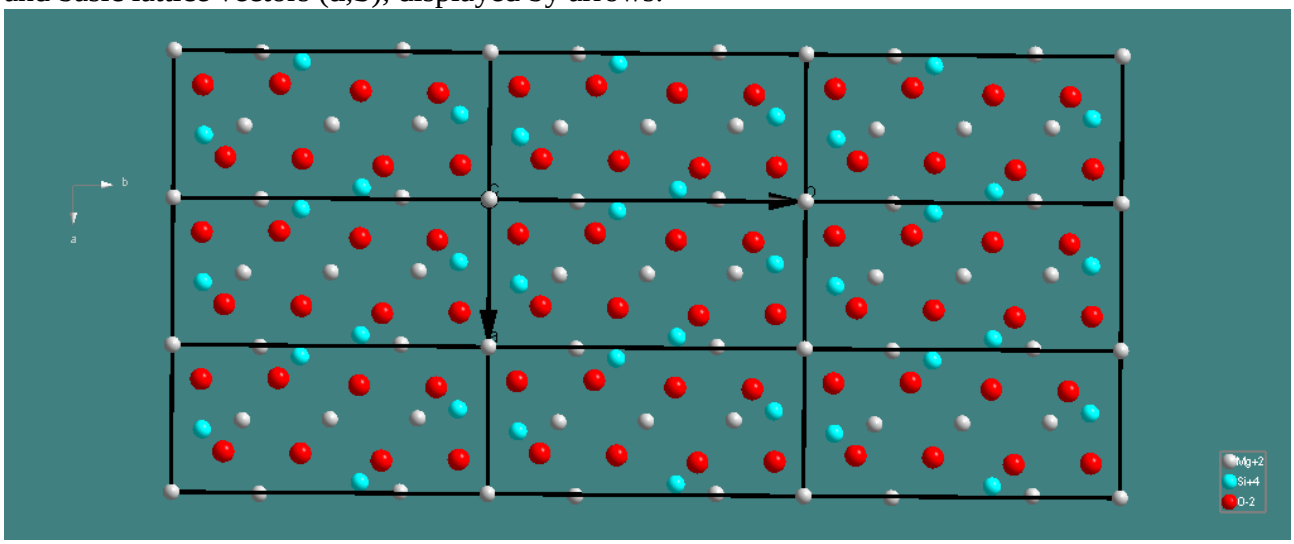

Crystal site: crystals host atoms at given positions; all this can be modelled by the notion of potential well. An elementary model to provide a depiction of a potential well is that borrowed from classic mechanics, and based on a spherical mass, suffering gravity and oscillating at the bottom of a pit

wherein it is confined. A crystal site is therefore a volume of a crystal where an atom can be potentially hosted, and confined.

Atoms do not stand at rest in a crystal: they oscillate at crystal sites, likewise masses constrained by springs that call them back to fixed points of space, *i.e*. *crystallographic coordinates*. The larger the temperature, the more atoms oscillate around their crystal coordinates. The energy of an atom can be split into two components: (1) kinetic contribution, which accounts for vibrational motion; (2) potential term that is responsible for the atom being bound to a given site. Providing thermal energy by heating, the kinetic contribution increases, leading to atomic oscillations more and more large.

Below it is shown the mechanic model which gives a rough but realistic depiction of the energy configuration at a crystal site.

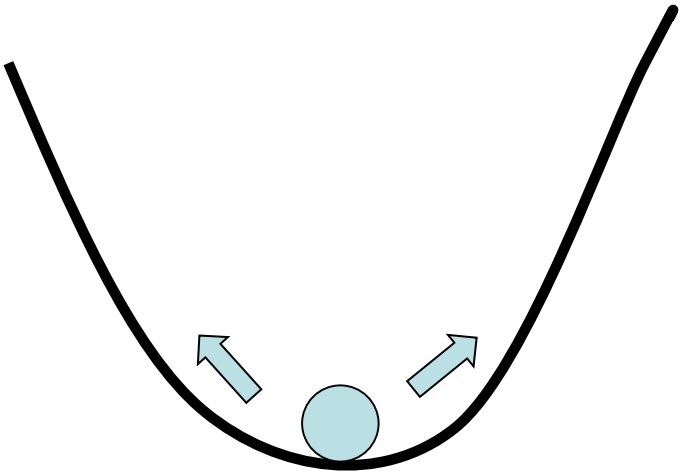

In this view, a crystal site is naturally associated with the notion of ‘’potential capacity’’ of constraining an atom within a given region of a crystal. Note that a crystal site may be occupied by different chemical species, as a function of their size (ionic radius), state of oxidation and temperature. The probability of having a given chemical species, Y, at a site, S, is called the "*occupancy of Y at S*". For instance, Fe and Mg are known to be able to occupy the same site; in such a case,

$P(\mathrm{Mg}) + P(\mathrm{Fe}) = 1$

where $P(\mathrm{Mg})$ and $P(\mathrm{Fe})$ are the probability coefficients to have Mg and Fe, respectively, at the site in question, and the sum of the occupancy factors at a given site must be equal to unity.

In an *ideal* crystal, if at **x** one has for instance Mg, then one keeps finding magnesium at any position such that **x**+**T**, where **T** is an arbitrary lattice translation. In the case of a description using occupancies, **x** is the position of a *site* that is characterised by a given $P(\mathrm{Mg})$, $P(\mathrm{Fe})$,….set of probability values of hosting Mg-Fe-etc.., respectively. This means that moving from **x** by a lattice vector, *i.e*. **x**+**T**, implies that one has *only a given probability* to find in the new site a specific chemical species.

In so doing, the *notion of occupancy*, allows one to describe the crystal structure by means still of the elementary cell that is translated by the lattice vectors. But the atoms are replaced, if needed, by the notion of site-occupancies according to a probabilistic scheme, which thing provides the basis underlying the solid solution formation mechanism.

By way of example, let us consider the simple and explanatory solid solution of fayalite [Fe_2SiO_4] and forsterite [Mg_2SiO_4]. One can approximately assume they have equal structure, but the former has Fe at given sites (called M-sites), whereas the latter bears Mg; Si and O occupy the same positions in both minerals. Mg and Fe easily replace one another, so that one may envisage a ‘’mixed’’ configuration in which the M-sites are not deterministically occupied by Fe or Mg, but each M-site shows just a probability of hosting magnesium or iron. This is somehow as though forsterite and fayalite ‘’mixed up’’ with one another, providing therefore a ‘’solid solution’’.

‘’Isomorphism’’ (similarity in form) is the particular condition in which two minerals have nearly the same structure, save for small changes of the atomic positions as a function of composition, *i.e.* relaxation that makes atoms readjust their coordinates in order to minimize the Gibbs energy. The fundamental notion underlying isomorphism is ‘’replacement of atoms with other atoms’’. We classically classified four types of isomorphism:

1) **First type**. Example: forsterite, Mg_2SiO_4, and fayalite, Fe_2SiO_4. One Mg is progressively replaced by one Fe, or vice-versa. In practice, atomic replacements involve one species *versus* one species (cations), only. That is Mg $\leftrightarrow$ Fe. Mg_2SiO_4 and Fe_2SiO_4 are called ‘’end members’’ of the solid solution. $(Mg_xFe_{1-x})SiO_4$ $0<x<1$, or $(Mg,Fe)_2SiO_4$.
2) **Second type**. Example: albite, $NaAlSi_3O_8$, and anortite, $CaAl_2Si_2O_8$. In this case, two species versus two species (cations) are involved, in order to preserve electroneutrality. That is $Na+Si \leftrightarrow Ca+Al$. $(Na_xCa_{1-x})(Al_{1+x}Si_{3-x})O_8$ $0<x<1$, or $(Na,Ca)(Al,Si)_4O_8$.
3) **Third type**. Example: rutile, TiO_2, and sellaite, MgF_2. That is $Ti + 2O \leftrightarrow Mg+2F$.
4) **Fourth type**. Example: nepheline, $NaAlSiO_4$, and cristobalite, $\square SiSiO_4$, where one has a replacement of $\square$ (vacancy) *versus* Na. That is $\square+Si \leftrightarrow Na+Al$.

Atomic replacement between cations, or anions, is favoured by:

- Similar ionic radii;
- Equal (similar) states of oxidation;
- High temperature, which makes sites more tolerant to accept diverse chemical species.

Cooling processes. Let us assume to have a melt constituted by given elemental species, and cool it down. What happens? In general, cooling down implies a reduction in terms of kinetic energy; as a consequence, the atoms involved become ever more sensitive to the inter-atomic interactions. We distinguish two cases for cooling processes:

(1) *slow cooling*, where thermal energy is subtracted slowly, and atoms have time to readjust one with respect to the others under the action of inter-atomic forces. Such a situation leads to the formation of crystals, *i.e.* ordered structures;
(2) *fast cooling*, where thermal energy is subtracted without leaving any chance to the system to relax properly and adjust its atoms under the action of the inter-atomic forces. This produces glass structures, without atomic ordering.

If one re-warms a glass sufficiently, it tends to develop crystals. This suggests that crystals represent a more stable state of solid-state matter than glass structures. Note that in nature, because of the duration of geologic processes (bar effusive rapidly cooling reactions), one reasonably expects to have crystals. This is the case of minerals.

In industrial transformations, conversely, the abrupt interruption of firing, favours the development of systems with large content of glass structures.

In short, one could say that ‘’it is a question of reaction kinetics’’. This is fully true!

II. **GROUPS**

An **<u>algebraic structure</u>** is constituted by a set of objects (elements), Ω, and a combination rule, ⊥, such that a⊥b=c, where c still belongs to Ω.
A ***<u>group</u>*** is a special case of algebraic structure. In particular, some rules hold:
1) it is defined an element, called the neutral element, n, such that ∀ a ∈ Ω then
a⊥n= n⊥a=a;
2) for any element, a, of Ω there exists an element a^{-1}, called the inverse element of a, such that
$a\perp a^{-1}= a^{-1}\perp a=n$;
3) the associative rule holds, that is a⊥b⊥c= (a⊥b)⊥c= a⊥(b⊥c).
Note that in general a⊥b≠ b⊥a. Those groups for which a⊥b=b⊥a are called ‘’**abelian**’’.

Subgroup: a subset of Ω whose elements still constitute a group is called a ‘’subgroup’’.

Examples.

1) Let us take the following matrices:

$$\begin{pmatrix}1&0&0\\0&1&0\\0&0&1\end{pmatrix},\ \begin{pmatrix}1&0&0\\0&-1&0\\0&0&1\end{pmatrix},\ \begin{pmatrix}-1&0&0\\0&-1&0\\0&0&-1\end{pmatrix},\ \begin{pmatrix}-1&0&0\\0&1&0\\0&0&-1\end{pmatrix}$$

They have the algebraic structure of a group with respect to the standard matrix-by-matrix product, which acts as combination rule. By the way, this group is also **abelian**!

2) Let us now take these other matrices reported below:

$$\begin{pmatrix}1&0&0\\0&1&0\\0&0&1\end{pmatrix},\ \begin{pmatrix}1&0&0\\0&-1&0\\0&0&-1\end{pmatrix},\ \begin{pmatrix}-1&0&0\\0&-1&0\\0&0&1\end{pmatrix},\ \begin{pmatrix}-1&0&0\\0&1&0\\0&0&-1\end{pmatrix}$$

They are a group with respect to the matrix-by-matrix product, but it is **not abelian**.

3) Let us take three conventional and non-coplanar vectors, **a**-**b**-**c**, and consider the set of {**T**}-vectors such that ∀ **t** ∈ {**T**} is expressed as $n\mathbf{a}+m\mathbf{b}+p\mathbf{c}$=t, where *n*-*m*-*p* are integers. {**T**}, in which one defines a combination rule according to the conventional summation of vectors, *i.e.* $\mathbf{t}_1 + \mathbf{t}_2 = (m_1+m_2)\mathbf{a}+(n_1+n_2)\mathbf{b}+(p_1+p_2)\mathbf{c}$, is an example of ***abelian*** group.

III. VECTORS IN 3D

Let us recall the notion of vectors as it is usually known, *i.e.* oriented segments in 3D-space. Such kind of vectors are hereafter addressed to as ‘’usual vectors’’.

Lengths and angles between vectors (3D)
The determination of lengths and angles between vectors is carried out as follows.
Let us start with vector length and assume $\{\mathbf{a}_j\}$ be a set of vectors that do not lie on the same plane, and therefore allow one to describe any other vector.
Then, if $\mathbf{v}=x_1\mathbf{a}_1+x_2\mathbf{a}_2+x_3\mathbf{a}_3$, one can write
$|\mathbf{v}|=\mathrm{sqrt}(\mathbf{v}^2)$
and therefore

$\mathbf{v}^2=(x_1\mathbf{a}_1+x_2\mathbf{a}_2+x_3\mathbf{a}_3)\cdot(x_1\mathbf{a}_1+x_2\mathbf{a}_2+x_3\mathbf{a}_3) = \sum_{j=1,n;\ i=1,n} x_i\, G_{ij}\, x_j$, $G_{ij}=\mathbf{a}_i\cdot\mathbf{a}_j$.

In matrix shape,
$X^T\,\mathbf{G}\,X = \mathbf{v}^2$,
where **G** is called metric matrix. In full,
$|\mathbf{v}|=\mathrm{sqrt}(X^T\,\mathbf{G}\,X)$. (1.a)

The angle between **u** and **v** is easily calculated from the scalar vector product. In fact, taking into account that
$\mathbf{u}\cdot\mathbf{v} = |\mathbf{u}|\,|\mathbf{v}|\cos(\mathbf{u}\hat{}\mathbf{v})$
one obtains
$\cos(\mathbf{u}\hat{}\mathbf{v}) = (\mathbf{u}\cdot\mathbf{v})/(|\mathbf{u}|\,|\mathbf{v}|)$.
Furthermore,

$(\mathbf{u}\cdot\mathbf{v}) = (x_1\mathbf{a}_1+x_2\mathbf{a}_2+x_3\mathbf{a}_3)\cdot(y_1\mathbf{a}_1+y_2\mathbf{a}_2+y_3\mathbf{a}_3) = \sum_{j=1,n;\ i=1,n} y_i\, G_{ij}\, x_j,$

$Y^T\,\mathbf{G}\,X = (\mathbf{u}\cdot\mathbf{v})$,
and hence

$$\cos(\mathbf{u}\hat{}\mathbf{v}) = Y^T\,\mathbf{G}\,X\,/(\,\mathrm{sqrt}(X^T\,\mathbf{G}\,X)\,\mathrm{sqrt}(Y^T\,\mathbf{G}\,Y)). \qquad (1.b)$$

Cell volume
Let **a**-**b**-**c** be three vectors not lying on the same plane and forming a *right-handed set*. They, then, determine a volume in 3D-space. The volume fixed by such vectors is easily calculated and can be expressed as
$V = \mathbf{a}\times\mathbf{b}\cdot\mathbf{c}$. Such a kind of product between vectors is known as a mixed-product.

A useful relationship, strictly linked to those above, is the following one:
$\det(\mathbf{G}) = V^2$.

IV. VECTOR SPACES

Vectors are "abstract" objects that in the present case will be made coincide with conventional oriented segments in 3D-euclidean space, *i.e.* ''usual vectors''. However, let us take them for a moment as "abstractions", and let us indicate each vector with a bold letter, *i.e.* **a b c**…. Let us address complex/real number by Greek letters, *i.e.* α β γ…...Let us eventually assume that are defined two combination rules:

(i) product between a number and a vector, so that a vector is produced ($\alpha\cdot\mathbf{a}$ is still a vector. In such a respect, you can think of the conventional multiplication rule between a number ad a usual vector);
(ii) sum of two vectors, so that a new vector is produced (**a** + **b** is still a vector. Let you consider the case of conventional combination rule of usual vectors adopting the parallelogram rule).

Vector space: a structure constituted by a set of object called vectors and the set of complex/real numbers, and such that are defined combination rules in order that
a + **b** = **b** +**a** is still a vector;
it exists a vector, **0**, such that **0**+**a**=**a**;
for each **a**, there exists a –**a** vector that **a**+(**-a**)=**0**;
and
$\alpha\cdot\mathbf{a}$ is still a vector (naturally $\alpha\cdot\mathbf{a}+\beta\cdot\mathbf{b}$ is a vector!),
$0\cdot\mathbf{a}=\mathbf{0}$. Note that in the following we drop the symbol ''·'', for the sake of brevity.

Examples

A first case is given by the usual vectors

A second case is the one in which vectors are *n*-component column arrays of real/complex numbers, *i.e.*

$$\begin{pmatrix}\alpha\\ \beta\\ \gamma\end{pmatrix},$$

and the combination rules are given by

$$\begin{pmatrix}\alpha'\\ \beta'\\ \gamma'\end{pmatrix}+\begin{pmatrix}\alpha''\\ \beta''\\ \gamma''\end{pmatrix}=\begin{pmatrix}\alpha'+\alpha''\\ \beta'+\beta''\\ \gamma'+\gamma''\end{pmatrix} \quad \text{and} \quad \lambda\begin{pmatrix}\alpha'\\ \beta'\\ \gamma'\end{pmatrix}=\begin{pmatrix}\lambda\alpha'\\ \lambda\beta'\\ \lambda\gamma'\end{pmatrix}.$$

Subspaces
They are subsets of vectors that preserve the properties of a vector space.

Linear combination of vectors
$\alpha\mathbf{a} + \beta\mathbf{b} + \gamma\mathbf{c}$……
is called a linear combination of vectors.

Linearly independent/dependent vectors
A set of vectors $\{\mathbf{a}_j\}=\mathbf{a}_1,\ldots,\mathbf{a}_n$ is said to be *linearly independent* if
$\sum_j \alpha_j \mathbf{a}_j = \mathbf{0} \Rightarrow \alpha_j = 0$.
Conversely, it is said *linearly dependent* if
$\sum_j \alpha_j \mathbf{a}_j = \mathbf{0} \Rightarrow$ at least one among $\{\alpha_j\}$ must be other than 0.

Basis
A ‘’basis’’ is a set of linearly independent vectors, {**a**} of a vector space, Ω, such that any vector of Ω is expressible as a linear combination of {**a**}. That is, given a basis $\{\mathbf{a}_1, \mathbf{a}_2, \ldots.\mathbf{a}_n\}$, and a generic vector **f** of Ω, then
$\mathbf{f} = \alpha_1 \mathbf{a}_1 +\ldots+ \alpha_n \mathbf{a}_n$. In the case of the usual vectors of the 3D, three vectors not laying in the same plane are a basis.

Linear transformations
Let us define a function that changes a vector of Ω into another one of Ω, *i.e.* $\mathbf{\Lambda}(\mathbf{v})=\mathbf{v'}$.
If
$\mathbf{\Lambda}(\alpha\,\mathbf{v})= \alpha\,\mathbf{\Lambda}(\mathbf{v})$
and
$\mathbf{\Lambda}(\mathbf{v}+\mathbf{v'})= \mathbf{\Lambda}(\mathbf{v}) + \mathbf{\Lambda}(\mathbf{v'})$
then **Λ** is a *linear mapping* of the vector space onto itself.

In the following we assume that given **Λ** there exists a $\mathbf{\Lambda}^{-1}$, such that
if $\mathbf{\Lambda}(\mathbf{v})=\mathbf{v'}$ then $\mathbf{\Lambda}^{-1}(\mathbf{v'})=\mathbf{v}$. In this case, one calls **Λ** a *bijective* application of the vector space into itself.

Matrices and linear transformations
Let us assume to have a basis set $\{\mathbf{a}_j\}$ of Ω (dimension=*n*), and a linear transformation **Λ**. Then one has

$$\mathbf{\Lambda}(\mathbf{u}) = \mathbf{\Lambda}\left(\sum_{j=1,n} x_j\mathbf{a}_j\right) = \sum_{j=1,n} x_j\,\mathbf{\Lambda}(\mathbf{a}_j) = \sum_{j=1,n;\ i=1,n} x_j\,L_{ij}\,\mathbf{a}_i \qquad (2.a)$$

where $\sum_{i=1,n} L_{ij}\,\mathbf{a}_i = \mathbf{\Lambda}(\mathbf{a}_j)$ and L can be likened to a $n\times n$ matrix.

Note that the equation above can be cast into a full-matrix form, that is

$\mathbf{\Lambda}(\mathbf{u}) = \{\mathbf{a}\}^T \mathbf{L}\, X$ (2.b)

where

$$\{\mathbf{a}\} = \begin{pmatrix} a_1 \\ .. \\ .. \\ a_n \end{pmatrix}, \{\mathbf{a}\}^T = \begin{pmatrix} a_1 & .. & .. & a_n \end{pmatrix}, X = \begin{pmatrix} x_1 \\ .. \\ .. \\ x_n \end{pmatrix}, \mathbf{L} = \begin{pmatrix} L_{11} & .. & .. & .. \\ .. & .. & .. & .. \\ .. & .. & .. & .. \\ .. & .. & .. & L_{nn} \end{pmatrix}$$

This demonstrates that matrices allow one to define univocally linear mappings. The matrix representing a linear mapping *depends* on the chosen basis. The necessary and sufficient condition (that we do not proof here) for $\mathbf{\Lambda}^{-1}$ to exist is that $\det(\mathbf{L}) \neq 0$, where **L** is the matrix representation of **Λ** in some basis.

Isometries

They are linear mappings that preserve the vectors' lengths, that is

$\mathbf{\Lambda}(\mathbf{u}) = \mathbf{u'}$ and $|\mathbf{u}| = |\mathbf{u'}|$. (3)

We do not prove the following statements, but it is important to keep in mind that:
in 3D, isometries are either ***rotations*** (**the matrix determinant is +1**) or ***reflections*** (rotoinversion, inversion and mirrors; **the matrix determinant is -1**).

Representation of linear mappings

It is trivial to represent a generic linear mapping, **Λ**, once one knows how it changes the reference axes. It is sufficient, on the basis of equ.(2.a), first to choose a given reference (**a**, **b**, **c**), then to write in the columns of the matrix the components of **Λ**(**a**), **Λ**(**b**), **Λ**(**c**) -first, second and third column respectively- as a function of **a**, **b**, **c**, *i.e.* for instance

$\mathbf{\Lambda}(\mathbf{b}) = \vartheta_1\mathbf{a} + \vartheta_2\mathbf{b} + \vartheta_3\mathbf{c}$

and therefore

$$\begin{pmatrix} \theta_1 \\ \theta_2 \\ \theta_3 \end{pmatrix}.$$

V. INVARIANCE OF LATTICES

Let us consider how is an isometry that changes a lattice into itself. In practical terms, we look for linear mappings such that

$\mathbf{\Lambda}(m\mathbf{a}+n\mathbf{b}+p\mathbf{c}) = m'\mathbf{a}+n'\mathbf{b}+p'\mathbf{c}$

where m, n, p, m', n', p' are integers, and for any given $m'\mathbf{a}+n'\mathbf{b}+p'\mathbf{c}$ there exists one $m\mathbf{a}+n\mathbf{b}+p\mathbf{c}$ that $\mathbf{\Lambda}(m\mathbf{a}+n\mathbf{b}+p\mathbf{c}) = m'\mathbf{a}+n'\mathbf{b}+p'\mathbf{c}$, *i.e.* **Λ** is *invertible*.

Fundamental equation

First of all, we analyse the structure of a matrix that represents an invertible linear mapping changing a lattice into itself, leaving aside any claim of having an isometry. In such a context, the matrix **L** associated to such a kind of transformation and expressed through the basis of the lattice vectors cannot but be formed by **integers**, to transform three integers into three integers. Moreover, given that there exists $\mathbf{L}^{-1}$, the inverse of a matrix has terms proportional to 1/det(**L**) and det(**L**) is an integer, then det(**L**) must be either 1 or -1. These conditions are very general.

Let now focus on *isometries* that do not change a lattice.
Given that equ.(1.a) must hold, then

$$\mathbf{\Lambda(u)}\cdot\mathbf{\Lambda(u)} = \mathbf{u'}\cdot\mathbf{u'}$$

and in matrix terms one has from equ.(2.a)

$$X^{T}\,\mathbf{G}\,X = (\mathbf{L}X)^{T}\,\mathbf{G}\,(\mathbf{L}X)$$

i.e.

$$X^{T}\,\mathbf{G}\,X = X^{T}\,\mathbf{L}^{T}\mathbf{G}\mathbf{L}\,X$$

and therefore

$$\mathbf{G} = \mathbf{L}^{T}\mathbf{G}\,\mathbf{L} \qquad (4)$$

That is the fundamental equation of isometries. It shows that for **L** to be a matrix of an isometry leaving unchanged a lattice whose metric is given by **G**, then **L** must fulfil equ.(4). Furthermore, **L** is constituted by integers.

Note that from equ.(4) it descends that $\det(\mathbf{L})^2=1$.

We skip the demonstration, but it is trivial to prove that the set of matrices **L**, satisfying equ.(4) for a given metric, form an algebraic group. Try to demonstrate it as an exercise! **Such groups are called *point groups* associated to a metric, and correspond to the point groups (symmetry classes) discussed of in the course of Mineralogy.**

One can conclude that should we be able to classify the possible metrics, then we could determine for each one the related group of isometries.

By way of example, let us assume to deal with a **G** matrix of the following type:

$$\begin{pmatrix} A & 0 & 0 \\ 0 & B & 0 \\ 0 & 0 & C \end{pmatrix}$$

$A=\mathbf{a}\cdot\mathbf{a}$, $B=\mathbf{b}\cdot\mathbf{b}$, $C=\mathbf{c}\cdot\mathbf{c}$, that is an **orthorhombic lattice**. In such a case, we have the following set of equations:

$$L_{11}^2\times A+L_{21}^2\times B+L_{31}^2\times C=A$$
$$L_{12}^2\times A+L_{22}^2\times B+L_{32}^2\times C=B$$
$$L_{13}^2\times A+L_{23}^2\times B+L_{33}^2\times C=C$$

Taking into account that *A*, *B*, *C* > 0 and that L_{ij}s are integers, then $L_{ii}^2=1$ and $L_{ik}=0$ if $i\neq j$.
Therefore, the matrices we are seeking for must have the following general structure:

$$\begin{pmatrix} \pm 1 & 0 & 0 \\ 0 & \pm 1 & 0 \\ 0 & 0 & \pm 1 \end{pmatrix}$$

Expanding the matrix above into all possibilities, one has:

$$M1=\begin{pmatrix} 1 & 0 & 0 \\ 0 & 1 & 0 \\ 0 & 0 & 1 \end{pmatrix}, M2=\begin{pmatrix} -1 & 0 & 0 \\ 0 & -1 & 0 \\ 0 & 0 & -1 \end{pmatrix}, M3=\begin{pmatrix} -1 & 0 & 0 \\ 0 & 1 & 0 \\ 0 & 0 & 1 \end{pmatrix}, M4=\begin{pmatrix} 1 & 0 & 0 \\ 0 & -1 & 0 \\ 0 & 0 & 1 \end{pmatrix}, M5=\begin{pmatrix} 1 & 0 & 0 \\ 0 & 1 & 0 \\ 0 & 0 & -1 \end{pmatrix},$$

$$M6=\begin{pmatrix} -1 & 0 & 0 \\ 0 & -1 & 0 \\ 0 & 0 & 1 \end{pmatrix}, M7=\begin{pmatrix} -1 & 0 & 0 \\ 0 & 1 & 0 \\ 0 & 0 & -1 \end{pmatrix}, M8=\begin{pmatrix} 1 & 0 & 0 \\ 0 & -1 & 0 \\ 0 & 0 & -1 \end{pmatrix}$$

One observes that:
M1->M8 form an algebraic structure, with respect to the usual matrix-by-matrix product, having the characters of a group (it is *mmm*);
It is possible to fix two sub-groups, represented by the matrices: (M1, M6, M3, M4. Corresponding to *mm2*) and (M1, M6, M7, M8. Corresponding to *222*).

Allowed rotations
We have stated above that the matrix representing a linear mapping, and an isometry as a particular case, depends on the basis vectors. Changing them, the matrix changes. We do not discuss the topic of "basis change" and its relations with the matrix of the linear mapping, but it suffices to keep in mind that matrixes of the same linear mapping, Λ, expressed in two bases, {**a'**} and {**a**}, *i.e.* **L**({**a'**}) and **L**({**a**}), are related to each other *via* the following equation:
$\mathbf{L}(\{\mathbf{a'}\})= \mathbf{S}\,\mathbf{L}(\{\mathbf{a}\})\,\mathbf{S}^{-1}$,
where S is a matrix allowing one to pass from {**a'**} to {**a**}. The important thing of the equation above is that:

- its trace is invariant, namely Tr(**L**({**a'**}))=Tr(**L**({**a**})). We recall here that the ''trace'' of a matrix is simply the sum of its diagonal terms;
- its determinant is invariant, namely det(**L**({**a'**}))=det(**L**({**a**})).

Once one has a matrix representing an isometry, it is immediate to classify it in terms of rotation or inversion by its determinant. Then, one has to take into account that, in the case of a rotation, it holds
$\mathrm{Tr}(\mathbf{L}) = 2 \times \cos(\alpha) + 1,$ (5)
where α is the rotation angle.

We now pay attention to **L** that changes a lattice into itself. Assuming **L** to be a rotation, *i.e.* det(**L**)=1, and taking into account that Tr(**L**) must be an integer, then

$2 \times \cos(\alpha) + 1 = n.$ (6)

Equ.(6) is fulfilled by a finite set of rotations, corresponding to α=360, 180, 120, 90, 60°, expressed by the notion of rotation order (*r*), *i.e.* **1**-**2**-**3**-**4**-**6** and in relation to 360/*r*=α.

Rotation order	Conversion	Angle
1	360/1	360
2	360/2	180
3	360/3	120
4	360/4	90
6	360/6	60

Isometry classification

One has often to classify a given matrix corresponding to a symmetry operation, which thing means to determine whether it is a rotation or a reflection (rotoinverion and plane), and to locate their positions.

Let us see how this is accomplished.

First of all, one must determine whether the operation in question is a rotation or a reflection. This is readily solved by calculating the determinant of the matrix. If it is 1, then we are dealing with a rotation, otherwise, that is -1, then we are facing with a reflection.

Then, if det=1, then it is a rotation, and one has to determine the rotation angle. This is an easy task! Let us calculate the matrix's trace, *i.e.* Tr, and use equ.(6).

Eventually, we have to determine the position of the rotation axis, or plane. In such a case, one should remind that the points lying on the rotation axis, or on the plane, are not changed by the transformation. This leads us to seek for those points that are left invariant by action of the symmetry transformation we are studying. Therefore, we have to solve the following equations

$$\begin{pmatrix} L_{11} & L_{12} & L_{13} \\ L_{21} & L_{22} & L_{23} \\ L_{31} & L_{32} & L_{33} \end{pmatrix} \begin{pmatrix} x \\ y \\ z \end{pmatrix} = \begin{pmatrix} x \\ y \\ z \end{pmatrix} \qquad (7)$$

The solution for *x*, *y* and *z* gives univocal indications about the position in the space of the symmetry operation we are treating.

Let us see some examples.

A)

$$\mathbf{M}=\begin{pmatrix} 0 & -1 & 0 \\ 1 & 0 & 0 \\ 0 & 0 & 1 \end{pmatrix}$$

Det(**M**)=1 $\rightarrow$ rotation

Tr(**M**)=1=2 × cos(α) + 1 → α=90°, *i.e*. n = 4. Note that at the present level of complexity we skip it to determine whether the rotation is clockwise or the reverse.
Using equ.(7),
$-y = x$
$x=y$
$z=z$.
The set of equations above leads one to state that
$x = y = 0$
and
z unconstrained.
Therefore, one concludes that the locus of points left invariant by the fourfold axis is the direction [0 0 1], formed by points whose coordinates are (0, 0, z).

B)

$$\mathbf{M}=\begin{pmatrix} 1 & 0 & 0 \\ 0 & -1 & 0 \\ 0 & 0 & 1 \end{pmatrix}$$

Det(**M**)=-1 → reflection

Using equ.(7),
$x = x$
$-y=y$
$z=z$.
The set of equations above leads one to state that
$y = 0$
and
z and x unconstrained.
Therefore, one concludes that the locus of points left invariant by the reflection has coordinates (x,0,z). This is simply the plane univocally determined by **a** and **c**.

C)

$$\mathbf{M}=\begin{pmatrix} 0 & 1 & 0 \\ -1 & 0 & 0 \\ 0 & 0 & -1 \end{pmatrix}$$

Det(**M**)=-1 → reflection.
Using equ.(7),
$y = x$
$-x=y$
$-z=z$.
The set of equations above leads one to state that
$x = y = z=0$.
Therefore, one concludes that the locus of points left invariant by the reflections shrinks to a single point (!!), corresponding to the origin, namely (0,0,0). The reflection cannot be a plane, but it is a rotoinversion. Now, given that the only one rotoinversion if -4, the problem is totally solved. Yet,

would one like to unravel such a problem in a smarter way, one should follow what is reported beneath.
Any rotoinversion, ***R***, is formed by two matrices:

R × **-1**

Where **R** is a rotation and -1 is a pure inversion, that is

$$\begin{pmatrix} -1 & 0 & 0 \\ 0 & -1 & 0 \\ 0 & 0 & -1 \end{pmatrix}.$$

We need to determine **R**. Therefore, one has to keep in mind that

R × **-1** = **R**.

In so doing, one attains

$$\mathbf{R} = \begin{pmatrix} 0 & -1 & 0 \\ 1 & 0 & 0 \\ 0 & 0 & 1 \end{pmatrix}$$

corresponding to the case of the example (**A**).
Altogether, we have that the matrix we are dealing with is a reflection and precisely a rotoinversion, whose rotation axis is fourfold, along [0 0 1].

VI. LATTICE TYPES

We have seen that the gist of the problem of determining all the symmetry classes is that we need to know the possible lattices. For one to properly take up such a question, we resort to three simple theorems, of hefty importance, which we shall skip to demonstrate.

Note that any lattice is invariant upon **-1**. In fact, it is trivial to observe that for any **r** lattice vector, there exists a **–r** lattice vector, too!

Three fundamental theorems

I) If a lattice is invariant for a rotation, then there exists a lattice row along the axis.
II) If a lattice is invariant for a rotation, then there exists a lattice plane normal to the axis.
III) If a lattice is invariant for a plane, then there exists a lattice row normal to the plane. Moreover, there must exist a two-fold axis normal to the plane. In such a view, the invariance upon a plane for a lattice reduces to the invariance upon a two-fold axis. Then, the presence of a two-fold axis entails that of a plane normal to it, too.

Let us now analyse the ‘’effects’’ of I , II and III, as a function of the rotation axis that leaves a lattice invariant. We can restrict our analysis to rotations in the light of the considerations above.

Note that our ensuing reasoning relies upon the notion of maximum-symmetry-axis, that is we start any discussion defining, first of all, the maximum order of rotation providing invariance to the lattice. In the following, we treat the classification of lattices by the notion that they are left unchanged by maximum-order-rotations with n=1, 2 (only one axis), 2(three axes), 4(only one axis), 3(only one axis), 6(only one axis), 4-3 (three 4-axes, or four 3-axes).

n=1
Only the 360°-rotation is present, which in practice corresponds to the unity-matrix. No constraint is set upon the lattice, whose metric matrix is totally unconstrained but its being symmetric. This case corresponds to ‘’**triclinic**’’ *crystal system*, with a metrics of the following type:

$$\begin{pmatrix} A & D & E \\ D & B & F \\ E & F & C \end{pmatrix}$$

$|\mathbf{a}|\neq|\mathbf{b}|\neq|\mathbf{c}|$
$\alpha\neq\beta\neq\gamma\neq 90°$

n=2
Let us assume to have only one 2-axis. One can take the **b**-axis along the rotation axis. Then, shortest period along the two-fold axis is used to determine univocally **b**. Given that a lattice plane is normal to the two-fold axis, one can find out two lattice vectors in the same plane, **a** and **c**; we take the shortest ones. This way, one has obtained a basis constituted by lattice vectors, and such that **b** is normal to **a** and **c**, while the angle between **a** and **c** is unconstrained. This one is the ‘’**monoclinic**’’ crystal system, with metrics

$$\begin{pmatrix} A & 0 & E \\ 0 & B & 0 \\ E & 0 & C \end{pmatrix}$$

$|\mathbf{a}|\neq|\mathbf{b}|\neq|\mathbf{c}|$
$\alpha=\gamma=90°$
$\beta\neq 90°$

Let us assume to have more than one 2-axis. In such a case, it might be proven that **three** twofold-axes must exist, and they are normal to each other. This implies that one can choose **a**-**b**-**c** as the shortest periods along the three 2-axes. The metrics results in

$$\begin{pmatrix} A & 0 & 0 \\ 0 & B & 0 \\ 0 & 0 & C \end{pmatrix}$$

$|\mathbf{a}|\neq|\mathbf{b}|\neq|\mathbf{c}|$
$\alpha=\gamma=\beta=90°$
The crystal system is ‘’**orthorombic**’’.

n=4

Let us assume to have <u>only one</u> 4-axis. One can, first of all, fix the shortest period along 4, and attribute to it the meaning of **c**-edge. Then, taking into account that there must needs exist a lattice plane normal to **c**, one seeks its shortest lattice vector, that is taken as **a**. Because of the 4-axis, there must exist a lattice vector rotated from **a** by 90-180-270° around **c**. We can choose the lattice vector rotated by either 90 or 270° as **b**, in order that it provides along with **a** and **c** a right-handed frame. Naturally, |**b**|=|**a**|. The metrics is in this case

$$\begin{pmatrix} A & 0 & 0 \\ 0 & B & 0 \\ 0 & 0 & B \end{pmatrix}$$

|**a**|=|**b**|≠|**c**|
α=γ=β=90°
The crystal system is ‘’**tetragonal**’’.

n=3

Let us assume to have <u>only one</u> 3-axis. One can, first of all, find the shortest period along 3, and attribute to it the meaning of **c**-edge. Then, taking into account that there must needs exist a lattice plane normal to **c**, one seeks its shortest lattice vector, that is taken as **a**. Because of the 3-axis, there must exist a lattice vector rotated from **a** by 120-240° around **c**. We can choose the lattice vectors rotated by either 120 or 240° as **b**, in order that it provides along with **a** and **c** a right-handed frame. Naturally, |**b**|=|**a**|. The metrics is in this case

$$\begin{pmatrix} A & D & 0 \\ D & B & 0 \\ 0 & 0 & B \end{pmatrix}$$

|**a**|=|**b**|≠|**c**|
α=β=90°
γ=120°
The crystal system is ‘’**trigonal**’’.

n=6

Let us assume to have <u>only one</u> 6-axis. This case is similar to the one just seen above. In fact, it is trivial to prove that a lattice plane invariant by a 3-axis, is invariant by a 6-axis, too. Therefore, the metrics appropriate for a lattice invariant to 3, can be transferred to that left unchanged by a 6. Hence:

$$\begin{pmatrix} A & D & 0 \\ D & B & 0 \\ 0 & 0 & B \end{pmatrix}$$

|**a**|=|**b**|≠|**c**|
α=β=90°
γ=120°

The crystal system is ‘’**hexagonal**’’.

Crystal systems hexagonal and trigonal are said to share the same **crystal family**, as they share the same set of lattice nodes, namely they fulfil the same metrics.

n=3 or n=4.
Let us assume to have more tha one 3-axis, or 4-axis. In such a case, one must have either four three-fold axes, or three four-fold axes. In both cases, it is possible to demonstrate that there must needs exist three two-fold axes normal to each other, with period vectors of the same length. Therefore, one can take as **a**-**b**-**c** three periods along the two-fold axes, having as short as possible a length. In this case, the metrics is

$$\begin{pmatrix} A & 0 & 0 \\ 0 & A & 0 \\ 0 & 0 & a \end{pmatrix}$$

$|\mathbf{a}|=|\mathbf{b}|=|\mathbf{c}|$
$\alpha=\beta=\gamma=90°$

The crystal system is ‘’**cubic**’’.

Note that just only one six-fold axis is allowed by the requirements to leave invariant a lattice.

In full, we have then **seven crystal systems**, and **six lattice systems (crystal families)**, the latter relatable to six metrics.

VII. POINT GROUPS

Now, given that we know that six metrics are possible, it is easy by means of equ.(4) to infer six sets of matrices, as satisfy the condition of having integers only. Each set corresponds to the largest set of symmetry operations that leave a given metrics unchanged.

For **triclinic** lattice system, we have a set composed of two matrices, *i.e.*

$$\begin{pmatrix} 1 & 0 & 0 \\ 0 & 1 & 0 \\ 0 & 0 & 1 \end{pmatrix}, \begin{pmatrix} -1 & 0 & 0 \\ 0 & -1 & 0 \\ 0 & 0 & -1 \end{pmatrix}$$

As already stated, they are a group that is addressed to as **-1**. It is trivial to observe that one can isolate a sub-set of matrices that still are a sub-group; in this case, it restricts to the identity matrix, and it is called **1**.

For **monoclinic** lattice system, we have a set composed of four matrices, *i.e.*

$$\begin{pmatrix}1&0&0\\0&1&0\\0&0&1\end{pmatrix},\begin{pmatrix}-1&0&0\\0&-1&0\\0&0&-1\end{pmatrix},\begin{pmatrix}1&0&0\\0&-1&0\\0&0&1\end{pmatrix},\begin{pmatrix}-1&0&0\\0&1&0\\0&0&-1\end{pmatrix}$$

They correspond to the **2/m** group. It is possible to recognise two subgroups, different from those of the triclinic, *i.e*.

$$\begin{pmatrix}1&0&0\\0&1&0\\0&0&1\end{pmatrix},\begin{pmatrix}1&0&0\\0&-1&0\\0&0&1\end{pmatrix}$$

called **m** group

and

$$\begin{pmatrix}1&0&0\\0&1&0\\0&0&1\end{pmatrix},\begin{pmatrix}-1&0&0\\0&1&0\\0&0&-1\end{pmatrix}$$

called **2** group.

One proceeds on with the other metrics, and in so doing one derives a total of **32** sets of matrices, called ***point groups***, compatible with the lattice systems obtained, according to the tables shown below:

CRYSTAL SYSTEM	LATTICE PARAMETERS	MAXIMUM SYMMETRY POINT GOUP
TRICLINIC	$a\neq b\neq c$ $\alpha\neq\beta\neq\gamma\neq 90°$	-1
MONOCLINIC	$a\neq b\neq c$ $\alpha\neq\gamma\neq 90°$ $\beta=90°$	2/m
ORTHOROMBIC	$a\neq b\neq c$ $\alpha=\gamma=\beta=90°$	mmm
TETRAGONAL	$a=b\neq c$ $\alpha=\gamma=\beta=90°$	4/mmm
HEXAGONAL	$a=b\neq c$ $\alpha=\beta=90°$ $\gamma=120°$	6/mmm
TRIGONAL		-3m
CUBIC	$a=b=c$ $\alpha=\gamma=\beta=90°$	m-3m

Lattice Systems	**Lattice parameters**	**Lattice symmetry= Maximum lattice symmetry**	**Sub-groups**
Triclinic	$a\neq b\neq c$ $\alpha\neq\beta\neq\gamma\neq 90$	-1	1
Monoclinic	$a\neq b\neq c$ $\alpha=\gamma=90$ $\beta\neq 90$	2/m	2, m
Orthorombic	$a\neq b\neq c$ $\alpha=\beta=\gamma=90$	mmm	mm2, 222
Tetragonal	$a=b\neq c$	4/mmm	4, -4, 4/m, 422, 4mm,

	α=β=γ=90		-42m
Hexagonal	*a*=*b*≠c α=β=90 γ=120	6/mmm	3, -3, 32, 3m, -3m, 6, -6, 6/m, 622, 6mm, -6m2
Cubic	*a*=*b*=c α=β=γ=90	m-3m	23, m3, 432, -43m

Therefore, each one of the 32 point groups is either a maximum-lattice-symmetry point group, or a sub-group of one of them.
Point groups are often called symmetry classes. See the table underneath:

1	Triclina pediale
-1	Triclina pinacoidale
2	Monoclina sfenoidica
m	Monoclina domatica
2/m	Monoclina prismatica
222	Ortorombica bisfenoidica
mm2	Ortorombica piramidale
mmm	Ortorombica bipiramidale
4	Tetragonale piramidale
-4	Tetragonale bisfenoidica
4/m	Tetragonale bipiramidale
422	Tetragonale trapezoedrica
4mm	Ditetragonale piramidale
-42m	Tetragonale scalenoedrica
4/mmm	Ditetragonale bipiramidale
3	Trigonale piramidale
-3	Trigonale romboedrica
32	Trigonale trapezoedrica
3m	Ditrigonale piramidale
-3m	Ditrigonale scalenoedrica
6	Esagonale piramidale
-6	Trigonale bipiramidale
6/m	Esagonale bipiramidale
622	Esagonale trapezoedrica
6mm	Diesagonale piramidale
-6m2	Ditrigonale bipiramidale
6/mmm	Diesagonale bipiramidale
23	Cubica tetraedrica-pentagonododecaedrica
m3	Cubica diacisdodecaedrica
432	Cubica pentagonoicositetraedrica
-43m	Cubica esacistetraedrica
m-3m	Cubica easacisottaedrica

They are represented by symbols known as Hermann-Mauguin symbols, representing the generators of a given point group. The generators are those elements that alone suffice to produce the others.

For instance:
In the case of the orthorhombic lattice, we have already derived the matrices of the maximum-lattice-symmetry point group (see exercise of section **V**, ‘’**Fundamental equation**’’). In full, we have eight matrices. Yet it is possible to reduce to three only, which generate the others by combination of one with another. The matrices representing the symmetry planes fulfil this requirement. Therefore, the symbol **mmm** means that the matrices related to three symmetry planes suffice to generate the whole group.

Why are the point groups so called?
Because they are represented by matrices that leave a common point of the space unchanged: it is (0,0,0). The term ‘’point’’ refers therefore to that that is not transformed by all the operations.

VIII. LATTICE CENTRING

We have derived the six lattice systems adopting the notion of maximum order rotation axis. This way, we have been able to fix up six metrics, each one associated with a given maximum symmetry point group, *via* equ.(4), from which its sub-groups descend. However, it is trivial to recognize that the lattices we have generated could be sub-lattices of node-richer lattices, the latter compatible with a given point group. We do not discuss the subject in depth, but it suffices that if one seeks possible lattices encompassing those we have built up and fulfilling their symmetry classes, then one discovers the ‘’***centred lattices***’’. They are lattices whose nodes include those of the six lattice systems, and are compatible with the related point groups.
For instance: let us take up the monoclinic lattice system, having **a**-**b**-**c**, as lattice vectors, and 2/m, as maximum symmetry point group. One might prove that the lattice whose nodes are obtained introducing the following additional vector
$\boldsymbol{\tau}$=½ **a** + ½ **b**
on one hand includes the original monoclinic lattice, on the other hand is still consistent with the operations of 2/m.
This means that 2/m is compatible to:
Primitive Monoclinic lattice, *i.e.* based on the standard vectors **a**-**b**-**c**. This lattice is addressed to as ‘’**primitive**’’ and represented by the character P;
Centred Monoclinic lattice, which uses an additional vector and is formed by more nodes than P. Such a lattice is known as ‘’**centred**’’, and the centring is of type ‘’C’’. It is obvious that the lattice C can be generated by a new set of lattice vectors ($\mathbf{a}_P$-$\mathbf{b}_P$-$\mathbf{c}_P$), which give all the C-nodes by a linear combination of integers.

In short:

- Primitive lattice corresponds to those lattice whose nodes are all obtained as n**a**+m**b**+p**c**;
- Centred lattice corresponds to those lattice requiring additional vectors with fractional coordinates, like $\boldsymbol{\tau}$. They can be reduced to primitive lattices by a change of the basis vectors, *i.e.* $\mathbf{a}_P$-$\mathbf{b}_P$-$\mathbf{c}_P$.

Skipping the demonstrations, we report beneath the possible centrings:

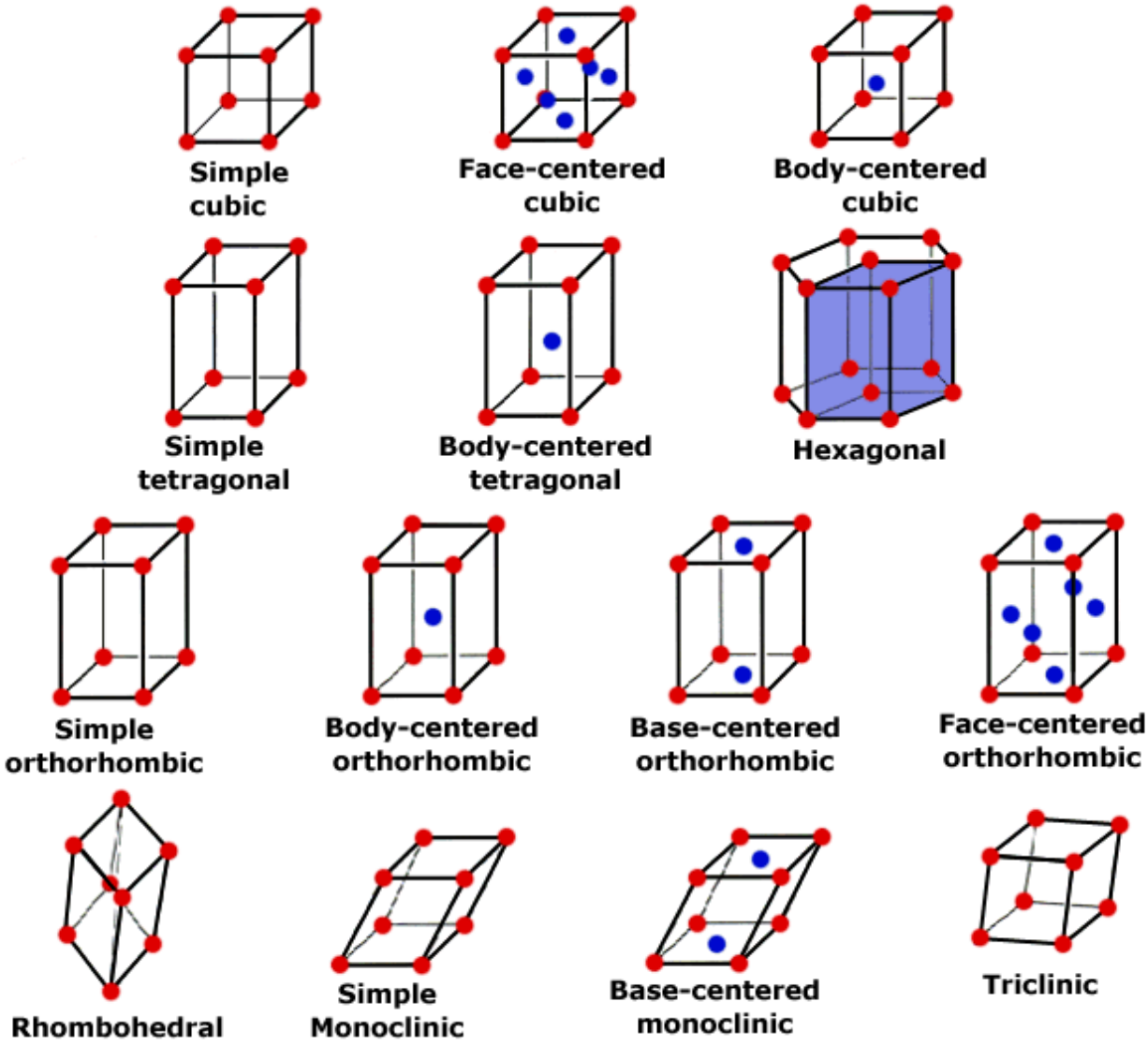

PRIMITIVE VECTORS	ADDITIONAL VECTORS	CENTRING NAME
a*-*b*-*c (triclinic)		
a*-*b*-*c (monoclinic)	1/2(***a***+***b***)	C
a*-*b*-*c (orthorombic)	1/2(***a***+***b***)	C
	1/2(***a***+***b***+***c***)	I
	1/2(***a***+***b***); 1/2(***a***+***c***); 1/2(***c***+***b***)	F
a*-*b*-*c (tetragonal)	1/2(***a***+***b***+***c***)	I
a*-*b*-*c (hexagonal; 6-order axis)	$\boldsymbol{a}_H$, $\boldsymbol{b}_H$, $\boldsymbol{c}_H$	P
a*-*b*-*c (rhombohedral; 3-order axis)	$\boldsymbol{a}_H/3$; $2/3\boldsymbol{a}_H+1/3\boldsymbol{b}_H+1/3\boldsymbol{c}_H$; $1/3\boldsymbol{a}_H+2/3\boldsymbol{b}_H+2/3\boldsymbol{c}_H$ $\boldsymbol{a}_H/3$; $1/3\boldsymbol{a}_H+2/3\boldsymbol{b}_H+1/3\boldsymbol{c}_H$; $2/3\boldsymbol{a}_H+1/3\boldsymbol{b}_H+2/3\boldsymbol{c}_H$	R
a*-*b*-*c (cubic)	1/2(***a***+***b***); 1/2(***a***+***c***); 1/2(***c***+***b***)	F
	1/2(***a***+***b***+***c***)	I

IX. SPACE GROUPS

Operations of space a space group

Until now, we have dealt with seeking the symmetry conditions that concern arrays of nodes, *i.e.* lattices. Let us assume that we would like to tackle the problem of the geometrical symmetry when a ‘’*motif*’’ replaces the simple nodes, generating a **crystal** and requiring that:

- The transformation we look for must turn the ‘’crystal’’ into itself;
- The translational invariance must keep on holding;
- The distance between two points is preserved upon transformation of the points in question;
- A lattice must change into itself.

We seek operations satisfying the conditions above and having the following structure:

{**R**|**T**+**t**}

where **R** is a rotation or reflection, **T** is a lattice translation (*i.e.* **T**=n**a**+m**b**+p**c**, n-m-p: integers) and **t** is a fractional translation (*i.e.* **t**=α**a**+β**b**+γ**c**, -1<α-β-γ<1).

Naturally

{**R**|**T**+**t**}(**x**)=**Rx**+**T**+**t** (8)

i.e.

$$\begin{pmatrix} R_{11} & R_{12} & R_{13} \\ R_{21} & R_{22} & R_{23} \\ R_{31} & R_{32} & R_{33} \end{pmatrix}\begin{pmatrix} x \\ y \\ z \end{pmatrix}+\begin{pmatrix} n \\ m \\ p \end{pmatrix}+\begin{pmatrix} \alpha \\ \beta \\ \gamma \end{pmatrix}.$$

Let us assume to have two transformations of the sort we have discussed above. How do they combine with one another? Let us see:

{**R’**|**T’**+**t’**}{**R**|**T**+**t**}(**x**)= { **R’**|**T’**+**t’**}(**Rx**+**T**+**t**)= **R’Rx**+ **R’T**+ **R’t**+ **T’**+**t’**=

={ **R’R**|**R’T**+**R’t**+ **T’**+**t’**}(**x**).

Note that {**R**|**T**+**t**} is a linear transformation no more!

Naturally:

-a pure lattice translation corresponds to the transformation given by {**I**|**T**}, *i.e.*

$$\begin{pmatrix} 1 & 0 & 0 \\ 0 & 1 & 0 \\ 0 & 0 & 1 \end{pmatrix}+\begin{pmatrix} n \\ m \\ p \end{pmatrix}$$

-a centring corresponds to {**I**|**t**}, *i.e.*

$$\begin{pmatrix} 1 & 0 & 0 \\ 0 & 1 & 0 \\ 0 & 0 & 1 \end{pmatrix}+\begin{pmatrix} \alpha \\ \beta \\ \gamma \end{pmatrix}$$

-the **R** component is a matrix of the point groups.

Space groups: general aspects and crystal structures

In full, we have **230** space groups, *i.e.* sets of transformation like (8) having the algebraic structure of a group.

X. GENERAL ASPECTS OF SCATTERING

Exponential complex numbers

A complex number is generally represented by
$c=a + i\ b$.
One can assume to report the real part of c, *i.e*. Re(c), on the X-axis, and its imaginary component, *i.e*. Im(c), on the Y-axis. This way c is represented as a vector of the Re-Im plane. We can then resort to usual *polar* coordinates. Hence, setting:
$\rho=\sqrt{a^2 + b^2}$
and
$\vartheta=\arctan(b/a)$,
then one has:
$a=\rho\times\cos(\vartheta)$
$b=\rho\times\sin(\vartheta)$,
and therefore
$c==\rho\times\cos(\vartheta)+i\ \rho\times\sin(\vartheta)=\rho\times[\cos(\vartheta)+i\ \sin(\vartheta)]$.
We now define:
$e^{i\vartheta}=\cos(\vartheta)+i\ \sin(\vartheta)$. (9)

The advantage of using the complex exponential notation is that it allows one to combine the basic trigonometric properties with the simplicity of manipulating exponentials. Namely:

$e^{i\vartheta}\times e^{i\alpha}=e^{i(\vartheta+\alpha)}$.
In full, a generic complex number, *c*, is representable as
$c=\rho\times e^{i\vartheta}$,
and
$c\times d=(\rho\times e^{i\vartheta})\times(\sigma\times e^{i\alpha})=(\rho\times\sigma)\times e^{i(\vartheta+\alpha)}$.

Scattering processes

Now, we aim to investigate scattering processes to infer features of condensed matter. Scattering processes are characterised by a general geometry whose features are:
A radiation for experiments (X-ray, neutrons, electrons);
A scatterer (a single crystal; powder; an amorphous system);
A detector, which collects the scattered radiation.

We distinguish between:
Elastic processes, in which the incident particles' energy is not changed by the interaction with the scatterer. That is no energy is exchanged between radiation and matter.
Inelastic processes, in which the diffused radiation has changed its energy, because matter has either given or absorbed energy of the incident beam.

Hereafter we shall deal with elastic processes only.

The incident radiation is described by a versor, $\mathbf{S}_i$, giving its direction and way, and a wavelength, λ. Note that wavelength is directly related to energy via the De Broglie relationship. Scattered radiation is represented by a versos $\mathbf{S}_f$, i.e. its direction and way, and a wavelength, λ, that is equal to the one

of the incident particles, as we are dealing with elastic processes. It is usual to introduce a new definition, for the vectors representing the process:
$\mathbf{K}_i = \mathbf{S}_i/\lambda$ and $\mathbf{K}_f = \mathbf{S}_f/\lambda$. For elastic processes, one has $|\mathbf{K}_i| = |\mathbf{K}_f|$. The angle between $\mathbf{K}_i$ and $\mathbf{K}_f$ is called ''scattering angle'', or ''diffusion angle'', and is addressed to by 2ϑ.

Diffraction is an elastic scattering process due to a crystal.

|

XI. DIFFRACTION FORMALISM

Fundamental expression

We have to skip some formal developments that would be required for a full grasp of the fundamentals of the scattering theory, and retain those aspects only which are of import to the practical use of the notions of diffusion. We underscore here that quantum mechanics leads to a description of microscopic particles by the notion of wave-function, $\Psi(\mathbf{x},t)$, such that , $\Psi(\mathbf{x},t)^* \times \Psi(\mathbf{x},t)$ is the *density of probability* of having a particle at position **x** and time *t*. $\Psi(\mathbf{x},t)^* \times \Psi(\mathbf{x},t)\, dV$ is in turn the *probability* to find a particle at time *t* in the volume d*V* centred on **x**.
Moreover, we suppose to deal with monochromatic incident beam, *i.e*. beams whose particles (photons-neutrons-electrons) have only one energy, with wavelength λ. We focus on X-ray, and in particular on photons with λ of the order of magnitude of Å.
In this view, any particle of an incident beam can be represented by
$\Psi(2\pi\mathbf{K}_i \cdot \mathbf{x})_i \propto e^{(2\pi i \mathbf{K}_i \cdot \mathbf{x})}$,
whereas a scattered beam is given by
$\Psi(2\pi\mathbf{K}_f \cdot \mathbf{x})_f \propto e^{(2\pi i \mathbf{K}_f \cdot \mathbf{x})}$.
Therefore, the probability that a photon, interacting with a crystal of volume V_{total}, changes from an initial state "i" to a final "f", $P(\mathbf{K}_i \rightarrow \mathbf{K}_f)$, can be expressed in terms of

$$P(\mathbf{K}_i \rightarrow \mathbf{K}_f) \propto \left| \int_0^{V_{total}} \Psi(\mathbf{x},t)_i^* \, \Im(\mathbf{x},t) \Psi(\mathbf{x},t)_f \mathrm{d}V \right|^2$$

where $\Im$ is an operator that represents the interaction between photons and matter. We need to formulate a reliable description of $\Im$. Leaving complex aspects of the scattering theory aside, we resort to the Larmor equation, to provide a justification for the approximate expression we shall use to describe $\Im$.
The Larmor equation formalises a particularly important properties of charged particles: if they suffer an acceleration, they emit electromagnetic waves. This effect, which can be predicted using the Maxwell equations in a classical context, is readily transferable to the case of photons diffusion. In fact, the incident electromagnetic field (*i.e*. incident photon beam) case electrons of a target to oscillate, thus becoming themselves sources of electromagnetic fields, the latter constituting the scattered signals. The Larmor equation results in:

$$\delta\wp = \frac{2}{3}\frac{\delta q^2 a^2}{c^3} = \frac{2}{3}\frac{1}{c^3}(\delta q \times \boldsymbol{a})(\delta q \times \boldsymbol{a})$$

where $\delta\wp$=diffused power due to δq; $\boldsymbol{a}$= acceleration vector of a charged particle; *c*=speed of light; δq=charge. Note that we can write $\delta q = \rho\, dV$, where $\rho(\mathbf{x})$ is the ***electron density***[1]. In so doing, we obtain the following Larmor equation:

[1] The electron density is a function such that
$\rho(\mathbf{x})\, dV$
Gives the number of electrons contained in a d*V*-volume around **x**. Naturally,
$\int \rho(x) dV = \text{electrons in } V$. Moreover, electron density is a periodic function of the lattice translations, and therefore

$$\delta\wp \propto \left(\frac{e\rho\ \mathrm{d}V \times \boldsymbol{E}}{m_e \rho\ \mathrm{d}V} \times e\rho\ \mathrm{d}V\right)^* \left(\frac{e\rho\ \mathrm{d}V \times \boldsymbol{E}}{m_e \rho\ \mathrm{d}V} \times e\rho\ \mathrm{d}V\right),$$

that gives

$$\delta\wp \propto \left(\frac{e\boldsymbol{E}\rho\ \mathrm{d}V}{m_e}\right)^* \left(\frac{e\boldsymbol{E}\rho\ \mathrm{d}V}{m_e}\right).$$

The equation above suggests that ρ might be a candidate to describe the average interaction between photon beam and scattering crystal. In light of this, we write

$$P(\mathbf{K}_\mathrm{i} \to \mathbf{K}_\mathrm{f}) \propto \left|\int_0^{V_{total}} e^{-2\pi i \mathbf{K}_\mathrm{i}\cdot\mathbf{x}}\, \rho(\mathbf{x}) e^{2\pi i \mathbf{K}_\mathrm{f}\cdot\mathbf{x}} \mathrm{d}V\right|^2 = \left|\int_0^{V_{total}} \rho(\mathbf{x})\, e^{2\pi i \mathbf{Q}\cdot\mathbf{x}} \mathrm{d}V\right|^2 = |\Phi(\mathbf{Q})|^2 \qquad (10)$$

where

$\mathbf{Q} = \mathbf{K}_\mathrm{f} - \mathbf{K}_\mathrm{i}$,

and $\mathbf{Q}$ is called "*momentum transfer*".

Fundamental integration

One can re-write $\Phi(\mathbf{Q})$ of equ.(10) in the following way

$$\sum\nolimits_{\mathbf{T}} \int_0^{V\mathbf{T}} \rho(\mathbf{x}) e^{2\pi i \mathbf{Q}\cdot\mathbf{x}}\, \mathrm{d}V, \qquad (11)$$

where the integration over V_{total} has been split into integrations over the sub-volume $V\mathbf{T}$s, each one corresponding to an elementary cell translated of $\mathbf{T}$ with respect to an origin (reference cell). Taking into account equ.(11), then we re-cast the expression above into

$$\sum\nolimits_{\mathbf{T}} \int_0^{V\mathrm{E}} \rho(\mathbf{x}+\mathbf{T}) e^{2\pi i \mathbf{Q}\cdot(\mathbf{x}+\mathbf{T})} \mathrm{d}V, \qquad (12)$$

which allows one to integrate over the reference elementary cell's volume, VE.

In short, $\Phi(\mathbf{Q})$ becomes

$$\Phi(\mathbf{Q}) = \sum\nolimits_{T} e^{2\pi i \mathbf{Q}\cdot\mathbf{T}} \times \int_0^{V\mathrm{E}} \rho(\mathbf{x}) e^{2\pi i \mathbf{Q}\cdot\mathbf{x}} \mathrm{d}V = \int_0^{V\mathrm{E}} \rho(\mathbf{x}) e^{2\pi i \mathbf{Q}\cdot\mathbf{x}} \mathrm{d}V \times \sum\nolimits_{\mathbf{T}} e^{2\pi i \mathbf{Q}\cdot\mathbf{T}}. \qquad (13)$$

Equ.(13) can then be split into two components:

$\Phi(\mathbf{Q}) = \Delta(\mathbf{Q}) \times F(\mathbf{Q})$,

where:

- $\Delta(\mathbf{Q}) = \sum_{\mathbf{T}} \exp(2\pi i \mathbf{Q}\cdot\mathbf{T})$, which depends on the "geometry" only;
- $F(\mathbf{Q}) = \int_{V\mathrm{E})} \rho(\mathbf{x}) \exp(2\pi \mathbf{Q}\cdot\mathbf{x})\, \mathrm{d}V$, which is a function of the chemical content of the elementary cell through the electron density. $F(\mathbf{Q})$ is called ***structure factor***.

Let us analyse them separately.

XII. STRUCTURE FACTOR

$\rho(\mathbf{x}) = \rho(\mathbf{x}+\mathbf{T})$,

where $\mathrm{T} = n\,\mathbf{a} + m\,\mathbf{b} + p\,\mathbf{c}$.

Naturally, the electron density is fully determined once it is known in the elementary cell.

The contribution of $\Delta(\mathbf{Q})$

It is easy to prove that

$$\Delta(\mathbf{Q}) = \sum_{n=0}^{N_a} e^{2\pi i \mathbf{Q}\cdot n\mathbf{a}} \times \sum_{n=0}^{N_b} e^{2\pi i \mathbf{Q}\cdot n\mathbf{b}} \times \sum_{n=0}^{N_c} e^{2\pi i \mathbf{Q}\cdot n\mathbf{c}}, \qquad (14)$$

where *Na-Nb-Nc* are the numbers of elementary cells forming the crystal along **a**-**b**-**c**. From algebra, we know that

$$\sum_{n=0}^{N} e^{2\pi i n\omega} = \frac{1 - e^{2\pi i\omega(N+1)}}{1 - e^{2\pi i\omega}}. \qquad (15)$$

In fact, one faces a summation of the type reported below

$$\sum_{n=0}^{N} x^n = 1 + x + x^2 + x^3 + \cdots$$

If one multiplies the sum above by (1-*x*), then

$$(1-x) \times \sum_{n=0}^{N} x^n = 1 + x + x^2 + x^3 + \cdots + x^N - x - x^2 - x^3 - \cdots - x^{N+1} = 1 - x^{N+1},$$

and using the expression shown above it descends that

$$\sum_{n=0}^{N} x^n = \frac{1 - x^{N+1}}{1 - x}.$$

Therefore,

$$\Delta(\mathbf{Q}) = \frac{1 - e^{2\pi i \mathbf{Q}\cdot\mathbf{a}(N_a+1)}}{1 - e^{2\pi i \mathbf{Q}\cdot\mathbf{a}}} \times \frac{1 - e^{2\pi i \mathbf{Q}\cdot\mathbf{b}(N_b+1)}}{1 - e^{2\pi i \mathbf{Q}\cdot\mathbf{b}}} \times \frac{1 - e^{2\pi i \mathbf{Q}\cdot\mathbf{c}(N_c+1)}}{1 - e^{2\pi i \mathbf{Q}\cdot\mathbf{c}}}.$$

Taking into account that we aim at calculating $|\Delta(\mathbf{Q})|^2$, then we have to analyze the behavior of functions like

$$\frac{1 - e^{2\pi i\omega(N_a+1)}}{1 - e^{2\pi i\omega}} \times \frac{1 - e^{-2\pi i\omega(N_a+1)}}{1 - e^{-2\pi i\omega}} \approx \left(\frac{\sin\big(\pi\omega(N+1)\big)}{\sin(\pi\omega)}\right)^2.$$

Such a function has its maxima for ω(*i.e.* **Q**·**a**, **Q**·**b**, **Q**·**c**)=integer, where it takes values equal to N^2; other *local* maxima occur at ω×(*N*+1)=integer+1/2. In this second case, if one sets **integer**=0,±1,…..,±*N*, then ω=(1/2,±1+1/2,….)/(*N*+1) and the function takes decreasing values of $1/\sin^2[\pi\times(1/2,\pm1+1/2,\ldots.)/(N+1)]$. For ω×(*N*+1)=integer and setting **integer**=0,±1,…..,±*N*, then the function under study has minima and its value is zero. The behavior of $|\Delta(\mathbf{Q})|^2$ is displayed below

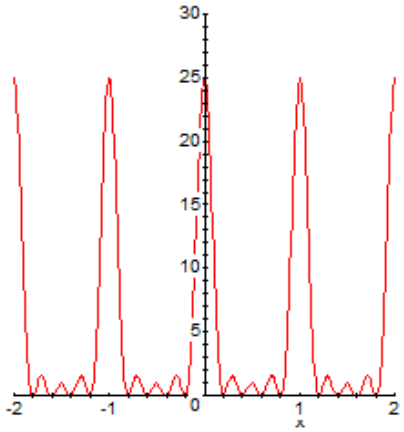

It is apparent that most of the diffraction intensity concentrates around momentum transfer vectors such that

$\mathbf{Q}\cdot\mathbf{a}=h$ (16.a)

$\mathbf{Q}\cdot\mathbf{b}=k$ (16.b)

$\mathbf{Q}\cdot\mathbf{c}=l$. (16.c),

h-k-l being integer, *i.e.* ω=integer.

This means that momentum transfer vectors that fulfil equ.(16a-b-c) provide the prominent contribution to diffraction. Such "special" **Q**s can be easily realized by means of *auxiliary vectors* that are commonly addressed to as ''*reciprocal vectors*'', and are formulated in terms of:

$\mathbf{a}^*=(\mathbf{b}\times\mathbf{c})/V_E$

$\mathbf{b}^*=(\mathbf{c}\times\mathbf{a})/V_E$

$\mathbf{c}^*=(\mathbf{a}\times\mathbf{b})/V_E$,

V_E,=elementary cell volume.

Note that:

$\mathbf{a}_m\cdot\mathbf{a}_n^*=\delta_{mn}$ (16.d)

where δ_{mn} is the Kroenecker symbol, that is 1 for m=n, and 0 otherwise.

Expanding (16.d), one has that

$\mathbf{a}\cdot\mathbf{a}^*=1$ $\mathbf{a}\cdot\mathbf{b}^*=0$ $\mathbf{a}\cdot\mathbf{c}^*=0$

$\mathbf{b}\cdot\mathbf{a}^*=0$ $\mathbf{b}\cdot\mathbf{b}^*=1$ $\mathbf{b}\cdot\mathbf{c}^*=0$

$\mathbf{c}\cdot\mathbf{a}^*=0$ $\mathbf{c}\cdot\mathbf{b}^*=0$ $\mathbf{c}\cdot\mathbf{c}^*=1$.

It is straightforward to prove the following relationship: $V^*=1/V_E$, where V^* is the volume of the reciprocal cell.

a*, **b*** and **c*** vectors are *unique*. This can be proven as follows. Let us assume one has determined a triple fulfilling eq.(16.d). We express then **a**, **b** and **c** as a function of **a***, **b*** and **c***. using the notation in which we introduce $\mathbf{a}_j$, j=1…3, in place of **a**, **b** and **c**, we write

$$\sum_{k=1,3} Z_{jk}\mathbf{a}_k^* = \mathbf{a}_j$$

If one multiplies both left- and right-hand side member of the equation above by $\mathbf{a}_m$, then

$$\sum_{k=1,3} Z_{jk}\mathbf{a}_k^*\cdot\mathbf{a}_m = \mathbf{a}_j\cdot\mathbf{a}_m$$

and using equ.(16.d) one obtains

$$\sum_{k=1,3} Z_{jk}\,\delta_{km} = \mathrm{G}_{jm}$$

i.e.

$$Z_{jm} = \mathrm{G}_{jm} \qquad (16.e),$$

and

$$\boldsymbol{Z} = \mathbf{G} \qquad (16.f)$$

$$\boldsymbol{Z^{-1}} = \mathbf{G^{-1}} \qquad (16.g).$$

Equ.(16.e-f-g) demonstrate that it is possible to find a unique linear transformation of the triple $\mathbf{a}_j$, into $\mathbf{a}_j$*, so that the relationship (16.d) holds.

Only momentum transfer vectors of the form

Q=*h* **a*** + *k* **b*** + *l* **c***

satisfy equ.(16a-b-c), diffraction processes' intensity concentrates around those directions. Moreover, **Q**s that are effective to diffraction form a lattice, known as ''*reciprocal lattice*'', and in such cases **Q** is usually replaced by the symbol **H**, to recall that it has *integer* coefficients.

Hereafter we use **H** to mean either

h **a*** + *k* **b*** + *l* **c***

or

$$\begin{pmatrix} h \\ k \\ l \end{pmatrix}.$$

Let us calculate the actual diffraction intensity associated with **Q=H**+δ, keeping in mind that diffraction occurs around **H**. In view of this, one expects that the intensity be proportional to the integration over a fraction centered on **H** of the reciprocal space, *i.e*.

$$I(\mathbf{H}) \propto \int |\Delta(\mathbf{H}+\delta)|^2 |F(\mathbf{H}+\delta)|^2 \mathrm{d}\delta$$

where $\delta=\eta_1 \mathbf{a^*} + \eta_2 \mathbf{b^*} + \eta_3 \mathbf{c^*}$, η's being small quantities, and $\mathrm{d}\delta = V^* \mathrm{d}\eta_1 \, \mathrm{d}\eta_2 \, \mathrm{d}\eta_3$. We skip here the full demonstration, which is presented by diffraction textbooks (see for instance a classic as Woolfson, 1997, An introduction to X-ray diffraction - second edition-Cambridge University Press), and show the final result below:

$$I(\mathbf{H}) \propto N \times V^* \times |F(\mathbf{H})|^2 = V_{\text{total-crystal}}/V^2 \times |F(\mathbf{H})|^2 \qquad (16.e)$$

where *N* is the number of unit cells in the crystal.

Symmetry of the reciprocal lattice

It is interesting to observe (leaving aside any demonstration) that the metric matrix of the reciprocal basis (**G***) is such that

$\mathbf{G^*} = \mathbf{G}^{-1}$.

Moreover, let us take up equ.(4) and change both right and left hand sides into their inverses, then one has

$\mathbf{G}^{-1} = \mathbf{L}^{-1}\mathbf{G}^{-1}\mathbf{L}^{\mathrm{T}-1}$

Given that the set of **L**-matrices is a group, the same holds for $\mathbf{L}^{\mathrm{T}}$s, and $\mathbf{L}^{-1}$ is still an element of the group in question, as well as $\mathbf{L}^{\mathrm{T}-1}$. Hence, whereas the **a**-**b**-**c** lattice is invariant for the **L**-operations, the **a**-**b**-**c** lattice is not changed by $\mathbf{L}^{\mathrm{T}}$s, *i.e.* the transposed matrices of the point groups'.

If one has to calculate |**H**|, then one can follow the same route for distance between two points. In other terms,

$$|\mathbf{H}|^2 = \mathbf{H}^T\,\mathbf{G^*}\,\mathbf{H} = \mathbf{H}^T\,\mathbf{G}^{-1}\,\mathbf{H} = (h \quad k \quad l)\begin{pmatrix} g_{11}^{-1} & g_{12}^{-1} & g_{13}^{-1} \\ g_{21}^{-1} & g_{22}^{-1} & g_{23}^{-1} \\ g_{31}^{-1} & g_{32}^{-1} & g_{33}^{-1} \end{pmatrix}\begin{pmatrix} h \\ k \\ l \end{pmatrix}. \qquad (17)$$

Bragg law

Let us consider the Bragg law, which has been proven earlier:

$$\frac{2}{|\mathbf{H}|}\sin(\vartheta) = \lambda \qquad \mathbf{H} = h\,\mathbf{a}^* + k\,\mathbf{b}^* + l\,\mathbf{c}^*$$

or

$2\,d_{hkl}\sin(\vartheta) = \lambda$.

It follows that

$|\mathbf{H}| = d_{hkl}^{-1}$

and by (17) we are now able to relate $\mathbf{G} \leftrightarrow \mathbf{G}^* = \mathbf{G}^{-1} \leftrightarrow |\mathbf{H}| \leftrightarrow d_{hkl} \leftrightarrow \vartheta$.
It is important to observe that d_{hkl} is determined as $1/|\mathbf{H}|$, the latter being the quantity that makes physical sense.

Let us see how this all practically works. From experiments, one is able to relate the ϑ-diffraction angle to $|\mathbf{H}|$, via the Bragg law, and to d_{hkl}^{-1}, then. Let us assume we have been successful to measure a set of
$hkl \leftrightarrow \vartheta \leftrightarrow d_{hkl}^{-1}$,
where the latter can be related to $\mathbf{H}^T\mathbf{G^*H}$. One changes the parameters of $\mathbf{G}^*$ (*i.e.* G^*_{ij}) until they give the best match between calculated and observed d_{hkl}^{-1}s. In so doing, the matrix $\mathbf{G^*}$ is determined and, by inversion, $\mathbf{G}$, too. As a consequence, one obtains the lattice parameters of a crystal. Note that we are only ''sketching'' the procedure. A first natural question would be: how can one attribute univocally a given diffraction peak to an *hkl*-vector? We skip this aspect that is rather technical, and suffices it to know that such a task is tackled by the *indexing-methods*.

Ewald's sphere

It is worthwhile presenting here a special construction known as ''**Ewald's sphere**''. In practice, the incident beam is represented along the AC segment (of length $1/\lambda$), in the picture below, whereas the diffracted beam travels along CP*. O*P* is the momentum transfer. The triangle AO*P* fulfils all the requirements of classic plane geometry. Naturally, only the reciprocal lattice points *lying* on the *Ewald's sphere* are able to contribute to diffraction, *i.e.* the riangle AO*P* gives the Bragg law. The Ewald's sphere can be rocked around O*, which is the origin of the reciprocal lattice, and in so doing one explores all the reciprocal points that are able to participate in diffraction. Rocking the Ewald's sphere is equivalent to rotating a single crystal, changing this way its orientation.

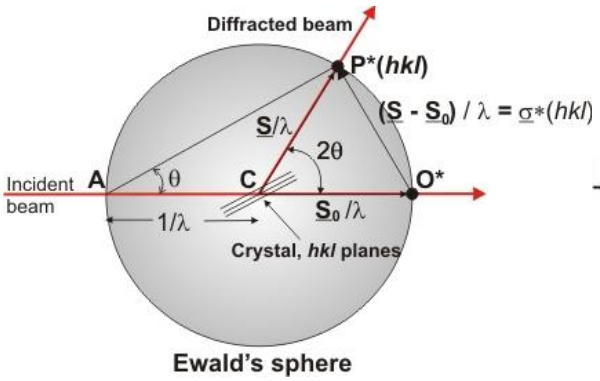

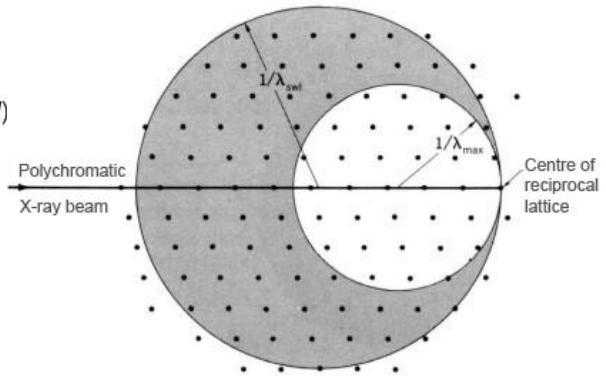

The contribution of $F(\mathbf{H})$

We would like to use electron density for specific atomic species. This is due to the fact that they have developed methods to calculate electron density of atoms, and it is a target of ours to discriminate in a structure between atoms of different chemical species. Let us use

$\rho(\mathbf{r})_j$

to indicate the electron density of an atom at the j-site, or belonging to the j-chemical species.
The picture beneath shows the electron density of some isolate atoms as a function of the distance from nucleus.

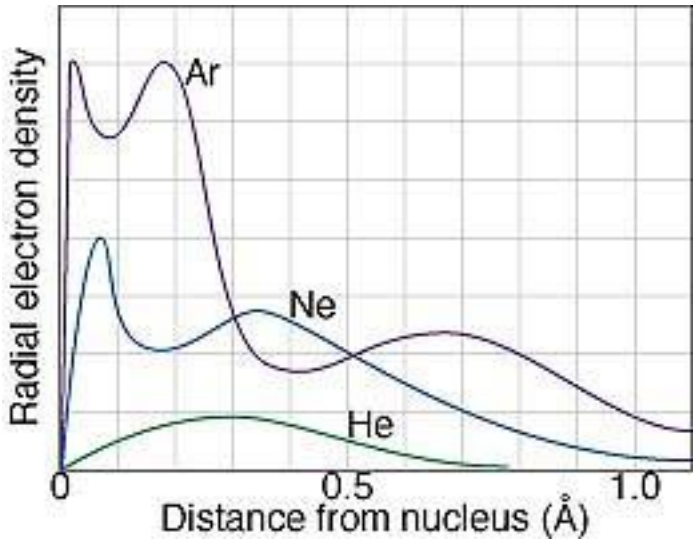

We would like to express $\rho(\mathbf{r})$ via $\rho(\mathbf{r})_j$. Note that the total electron density of a crystal is due to the atomic electron densities that superimpose each other. We would like to underscore anyway that it is not only a matter of superposition, as atoms interact with each other and change electron density accordingly. To understand this notion, let us look at the pictures reported beneath and showing qualitatively the complex structure of $\rho(\mathbf{r})$.

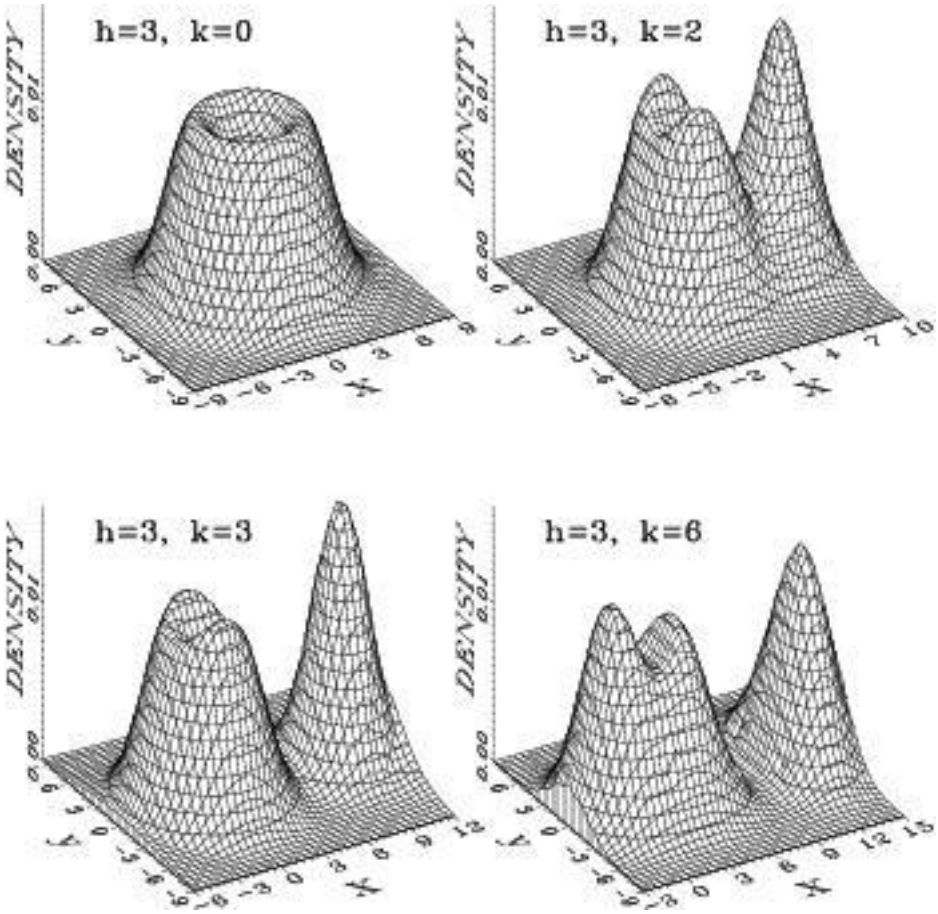

Let us think of having an atom at the j-site; if $\rho(\mathbf{r})_j$ is its electron density referred to the isolated atom, then its contribution to the general electron density at **r** will be:
$\rho(\mathbf{r}-\mathbf{r}_j)_j$.
This means that
$\rho(\mathbf{r}) = \sum_{j=1}^{atoms\ in\ cell} \rho(\mathbf{r}-\mathbf{r_j})_j$,
and

$$F(\mathbf{Q}) = \int_0^{VE} \rho(\mathbf{x}) e^{2\pi i \mathbf{Q}\cdot\mathbf{x}} \mathrm{d}V = \sum_{j=1}^{atoms\ in\ cell} e^{2\pi i \mathbf{Q}\cdot\mathbf{x}_j} \int_0^{VE} \rho(\mathbf{y}) e^{2\pi i \mathbf{Q}\cdot\mathbf{y}} \mathrm{d}V \qquad (18)$$

Now, we analyse

$$f(\mathbf{Q})_j = \int_0^{VE} \rho(\mathbf{y})_j \, e^{2\pi i \mathbf{Q}\cdot\mathbf{y}} dV \approx \int_0^{\infty} \rho(\mathbf{y})_j \, e^{2\pi i \mathbf{Q}\cdot\mathbf{y}} dV$$

that is the Fourier transform of the atomic electron density; $f(\mathbf{Q})$ is commonly called ''X-ray scattering power''. It can be proven that if the electron density is radial, *i.e*. it depends on the *length* of **y** only, then the integration in question simplifies significantly. Such an approximation though heavy is plausible, and sufficiently models the phenomenology we are investigating. Hence, if
$\rho(\mathbf{y})_j = \rho(|\mathbf{y}|)_j$,
then
$f(\mathbf{Q})_j = f(|\mathbf{Q}|)_j$, too. For each chemical species, the related $f(\mathbf{Q})$-function has been modelled, and parametrised as follows:

$$f(|\mathbf{Q}|) = f(|\mathbf{H}|) = \sum_{k=1,4-6} a_k e^{-\left(\frac{\sin(\vartheta)}{\lambda}\right)^2 b_k} + c_0 \qquad (19)$$

where we have taken into account that **Q** corresponds to a reciprocal lattice vector, *i.e.* **H**, and by the Bragg law it holds: $|\mathbf{H}|=2\sin(\vartheta)/\lambda$. The *a-b-c* parameters are available from the International Tables of Crystallography, or from the Internet.

In equ.(18), we need to analyse $exp(2\pi i\mathbf{Q}\cdot\mathbf{x}_j)$. $\mathbf{x}_j$ is the *instantaneous* position of the j-atom and changes as a function of time given that all atoms vibrate in a crystal. However, they can reasonably be assumed to vibrate around an *average position*, let us call it $\mathbf{x}_{j0}$. Then, we write

$\mathbf{x}_j=\mathbf{x}_{j0}+\boldsymbol{\Delta}_j$,

where $\boldsymbol{\Delta}_j$ accounts for a shift from the average position. Given that $|\boldsymbol{\Delta}|$ is small, then

$$e^{2\pi i\mathbf{Q}\cdot(\mathbf{x}_{j0}+\Delta_j)} = e^{2\pi i\mathbf{Q}\cdot\mathbf{x}_{j0}}e^{2\pi i\mathbf{Q}\cdot\Delta_j} \approx e^{2\pi i\mathbf{Q}\cdot\mathbf{x}_{j0}} \times \left[1 + 2\pi i\mathbf{Q}\cdot\Delta_j - 2\pi^2\left(\mathbf{Q}\cdot\Delta_j\right)^2 + \cdots\right]. \qquad (20)$$

During an experiment, one measures average quantities over time, due to the fact that a detector takes a given time to record a scattered signal. Therefore, we "time-average" the terms in equ.(20), obtaining:

$<\mathbf{Q}\cdot\boldsymbol{\Delta}_j>=0$,

and

$2\pi^2<(\mathbf{Q}\cdot\boldsymbol{\Delta}_j)^2>=2\pi^2\,\mathbf{Q}^2\times<\boldsymbol{\Delta}_j^2\times\cos^2\vartheta>= 2\pi^2\,\mathbf{H}^2\times<\boldsymbol{\Delta}_j^2>\times<\cos^2\vartheta>_j =(\sin(\vartheta)/\lambda)^2\times B_j$, where the last step is obtained by keeping in mind the Bragg equation.

Therefore, we from (20) have

$$e^{2\pi i\mathbf{Q}\cdot\mathbf{x}_{j0}} \times \left[1 - 2\pi^2\left(\mathbf{Q}\cdot\Delta_j\right)^2\right] \approx e^{2\pi i\mathbf{Q}\cdot\mathbf{x}_{j0}} \times e^{-\left(\frac{sen(\vartheta)}{\lambda}\right)^2 B_j}$$

where $exp(-(\sin(\vartheta)/\lambda)^2\times B)$ is called *Debye-Waller factor*, and B accounts for the atomic displacement owing to *thermal vibrations*. It becomes larger with increasing temperature, and depends on each atom. Naturally, $B>0$.

Putting together (18)-(19)-(20), one has

$$F(\mathbf{H}) = \sum_{j=1,atoms\ in\ cell} f\left(\frac{\sin(\vartheta)}{\lambda}\right)_j e^{2\pi i\mathbf{H}\cdot\mathbf{x}_{j0}} e^{-\left(\frac{\sin(\vartheta)}{\lambda}\right)^2 B_j} \qquad (21)$$

Equ.(21) represents the expression commonly used to calculate structure factors, and relies upon the spherical approximation of the atomic electron density. A more detailed treatment of the atomic electron density leads to the introduction of <u>two further terms</u> to describe the scattering power, that is $f(\lambda)$' and $f(\lambda)$'', so that one has in full:

$f(\sin(\vartheta)/\lambda)_j+f(\lambda)'_j+i\,f(\lambda)''_j$.

$f(\lambda)$' and $f(\lambda)$'' are called "*anomalous*" components. A qualitative way to better understand the origin of the anomalous components is provided by considering the equation of motion of a charge particle, *q*, suffering an electro-magnetic field as affected by a dumping-dissipative term, *i.e.*

$$q\vec{E} = m\vec{a} + \gamma\vec{v}$$

Leaving any detail aside, the component *f*'' is associated with absorption of electro-magnetic waves, and the behaviour of f' and f'' with respect to λ is shown by the figure below:

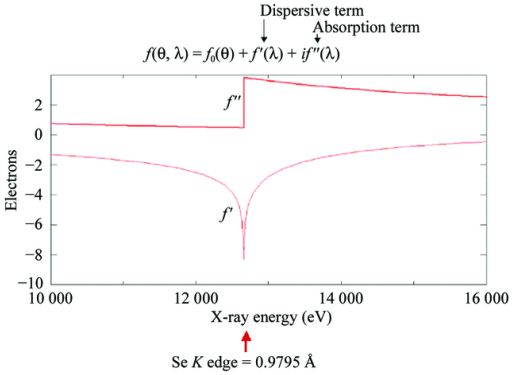

Note that the anomalous components are independent of the scattering angle, *i.e*. 2ϑ, at variance with *f,* whereas they are sensitive to the photon wavelength. This feature makes the anomalous scattering a phenomenon that can be used to differentiate the scattering contributions of *quasi*-isoelectronic species. In fact, such atoms have very similar *f*s, whilst they differ from each other in terms of *f*' and *f*''. In particular, it is possible to exploit the resonance properties of *f*' and *f*'' as a function of λ.

Therefore, one has to remind from (10), at a first level of approximation, that
$I(\mathbf{H})_{\text{experiment}} \propto |F(\mathbf{H})|^2$.
where *I* is the intensity observed in experiments for a momentum transfer **H**.

F(**H**) bears *three kinds of information*:
1) geometrical, related to the average atomic positions (*i.e*. *crystallographic positions*, those that we are able to observe experimentally) $\mathbf{x}_{j0}$;
2) physical, related to the atomic displacement parameters and atomic dynamics;
3) chemical, related to the scattering power that depends on the chemical species lying in a site.
Note that |*F*(**H**)| decreases upon increasing the scattering angle (ϑ) and temperature.

Eventually, let us write (21) in a more practical fashion. Given that $\mathbf{H}= h\,\mathbf{a}^* + k\,\mathbf{b}^* + l\,\mathbf{c}^*$, we can express the positions of atoms in the elementary cell as $\mathbf{x}_{j0}=x_{j0}\ \mathbf{a}+ y_{j0}\,\mathbf{b}+ z_{j0}\,\mathbf{c}$; in so doing and taking into account (16.d), one cast (21) into

$$F(\mathbf{H}) = \sum_{j=1,atoms\ in\ cell} f\left(\frac{\sin(\vartheta)}{\lambda}\right)_j e^{2\pi i(x_{j0}h+y_{j0}k+z_{j0}l)} e^{-\left(\frac{\sin(\vartheta)}{\lambda}\right)^2 \mathrm{B}_j} \qquad (22)$$

in which we explicitly use *fractionary crystallographic coordinates*, referred to the lattice translation vectors, *i.e*. the edges of the elementary cell.

Structure factors and electron density

Given that the electron density is a periodic function endowed of the lattice translational invariance, see equ.(11), then it can be expanded as a *Fourier series*.
We remind here that a generic function, $f(\mathbf{x})$, such that $f(\mathbf{x}+\mathbf{T})=f(\mathbf{x})$, where $\mathbf{T}=n\,\mathbf{a}+m\,\mathbf{b}+p\,\mathbf{c}$, can be represented *via* the following expansion

$$f(\mathbf{x}) = \frac{1}{V}\sum_{hkl=-\infty,+\infty} A_{hkl} e^{-2\pi i(hx+ky+lz)} \qquad (23.\text{a})$$

where *h,k,l* are integers and *x,y,z* are coordinates in the crystallographic cell. Moreover
$A_{hkl}=\int f(\mathbf{x}) e^{2\pi i(hx+ky+zl)}\,\mathrm{d}V$, (23.b)
the integration being carried out over the crystallographic cell volume. Taking into account equ.(23.b) and (18), then one can write
$\rho(\mathbf{x}) = \sum F(hkl) e^{-2\pi i(hx+ky+zl)} = \sum F(\mathbf{H}) e^{-2\pi i \mathbf{H}\cdot\mathbf{x}}$. (24)
The equation above demonstrates that the structure factors are directly related to the electron density. One could at first sight believe that by an experiment, where we can measure intensities and thereby the module of structure factors, it is possible to reconstruct the structure of a crystal. This is *incorrect*, as from intensity measurements we are not able to get the full information about structure factors, but their *modules* only. In other terms, the ***phase*** of each *F*(**H**) is unknown, from diffraction experiments based on the kinetic theory that is being presented here. In fact,
$F(\mathbf{H}) = |F(\mathbf{H})| \times e^{i\varphi}$
where φ is the ''***phase***'', which cannot be unearthed by the technique hitherto shown. Such a limit is overcome by resorting to the dynamic theory of diffraction, which do not treat here.

The information about structure that one can retrieve from diffraction intensities relies on the use of the *Patterson function*. Let us introduce the following function

$\Xi(\mathbf{x}) = \frac{1}{V}\int \rho(\mathbf{y})\rho(\mathbf{y}+\mathbf{x})dV_{\mathbf{y}}$

integrated over the cell volume. $\Xi(\mathbf{x})$ takes its maximum if **x** is an *inter-atomic vector*, such that connects a couple of atoms. $\Xi(\mathbf{x})$ is called "convolution", or "folding" and it is periodic. Its Fourier-type expansion, one can easily demonstrate, is

$$\Xi(\mathbf{x})=\sum_{H=-\infty}^{\infty} F(\mathbf{H}) \times F(-\mathbf{H}) \times e^{2\pi i(hx+ky+lz)} = \sum_{H=-\infty}^{\infty} |F(\mathbf{H})|^2 \times e^{2\pi i(hx+ky+lz)}. \quad (25)$$

Equ.(25) proves that experimental data, $I(\mathbf{H})$, allow one to determine the Patterson function only, and *not* the full electron density.

XIII. EXTINCTION and OTHER EFFECTS

Systematic extinctions

Let us assume that $\{\mathbf{R}|\mathbf{t}\}$ *be an operation of the space group* to which the crystal on study belongs. Then, it can be proven that:

$F(\mathbf{R}^{\mathrm{T}}\mathbf{H}) = F(\mathbf{H}) \exp(-2\pi i\, \mathbf{H}\cdot\mathbf{t})$. (26)

where $\mathbf{R}^{\mathrm{T}}\mathbf{H}$ means

$$\mathbf{R}^{\mathrm{T}}\mathbf{H} = \begin{pmatrix} R_{11} & R_{21} & R_{31} \\ R_{12} & R_{22} & R_{32} \\ R_{13} & R_{23} & R_{33} \end{pmatrix} \begin{pmatrix} h \\ k \\ l \end{pmatrix} = \begin{pmatrix} h' \\ k' \\ l' \end{pmatrix}$$

that is one replaces *hkl* in (22) with *h'k'l'*.
For the sake of simplicity, we often use the following notations:
$\mathbf{H}\,\mathbf{R}\,\mathbf{x} =$

$$= \mathbf{H}^{\mathrm{T}}\,\mathbf{R}\,\mathbf{x} = (h \quad k \quad l) \begin{pmatrix} R_{11} & R_{12} & R_{13} \\ R_{21} & R_{22} & R_{23} \\ R_{31} & R_{32} & R_{33} \end{pmatrix} \begin{pmatrix} x \\ y \\ z \end{pmatrix} = \mathbf{x}^{\mathrm{T}}\,\mathbf{R}^{\mathrm{T}}\mathbf{H} = (x \quad y \quad z) \begin{pmatrix} R_{11} & R_{21} & R_{31} \\ R_{12} & R_{22} & R_{32} \\ R_{13} & R_{23} & R_{33} \end{pmatrix} \begin{pmatrix} h \\ k \\ l \end{pmatrix}$$

and

$$\mathbf{H}\cdot\mathbf{t} = \mathbf{H}^{\mathrm{T}}\mathbf{t} = (h \quad k \quad l) \begin{pmatrix} x \\ y \\ z \end{pmatrix}$$

where we drop the explicit mention to whether we are using a full vector representation ($\mathbf{H}\cdot\mathbf{t}$) or we refer to the components only ($\mathbf{H}^{\mathrm{T}}\mathbf{t}$).

The demonstration is presented below. We have to introduce a particular representation of $F(\mathbf{H})$. First of all, we have to analyse some particular properties of sub-group and group. Let us assume that $\mathbf{W}_j$ is a symmetry operator of a group Ω, of order *M*, acting upon a point with coordinate **x**, then $\mathbf{W}_j\mathbf{x}=\mathbf{x'}$.
The set of $\{\mathbf{W}_j\}$that do not change **x** constitutes a sub-group of Ω of order *n*, and such that
$M=n\times\{1+$number of operators changing $\mathbf{x}\}$.
If $\mathbf{x}_{Ak}$ is the coordinate of the kth-atom of the <u>*asymmetric unit*</u> (AU), then we can re-write the structure factor in terms of

$$F(\mathbf{H}) = \sum_{j=1,atoms\ in\ cell} f_j\, e^{2\pi i \mathbf{H}\cdot\mathbf{x}_j} e^{-(\mathbf{H}^2/4)\mathrm{B}_j}$$
$$= \sum_{k=1,atoms\ in\ AU} f_{Ak} e^{-(\mathbf{H}^2/4)\mathrm{B}_j} \times \frac{n}{M} \sum_{l=1,M} e^{2\pi i \mathbf{H}^{\mathrm{T}}\mathbf{W}_l\mathbf{x}_{Ak}}$$

Let us see what happens in the case of $\mathbf{R}^{\mathrm{T}}\,\mathbf{H}$. The equation above changes into

$$F(\mathbf{R}^{\mathrm{T}}\mathbf{H}) = \cdots \sum_{l=1,M} e^{2\pi i (\mathbf{R}^{\mathrm{T}}\mathbf{H})^{\mathrm{T}}\mathbf{W}_l\mathbf{x}_{Ak}} = \cdots \sum_{l=1,M} e^{2\pi i \mathbf{H}^{\mathrm{T}}\mathbf{R}\mathbf{W}_l\mathbf{x}_{Ak}}$$

Taking into account that $\{\mathbf{R}\,|\,\mathbf{t}\}$, then

$\mathbf{R}\,\mathbf{W}_l = \mathbf{R}\,\mathbf{R}_l + \mathbf{R}\,\mathbf{t}_l + \mathbf{t} - \mathbf{t} = \{\,\mathbf{R}\,\mathbf{R}_l \mid \mathbf{R}\,\mathbf{t}_l + \mathbf{t}\,\} - \mathbf{t} = \mathbf{W}_u - \mathbf{t}$

and on the basis of the expression above one concludes that

$$F(\mathbf{R}^{\mathrm{T}}\mathbf{H}) = \cdots \sum_{l=1,M} e^{2\pi i \mathbf{H}^{\mathrm{T}}\mathbf{R}\mathbf{W}_l\mathbf{x}_{Ak}} = \cdots \ldots \sum_{u=1,M} e^{2\pi i \mathbf{H}^{\mathrm{T}}\mathbf{W}_u\mathbf{x}_{Ak}} \times e^{-2\pi i \mathbf{H}\cdot\mathbf{t}} = F(\mathbf{H}) e^{-2\pi i \mathbf{H}\cdot\mathbf{t}}$$

Q.E.D.

Note that:

1) $|F(\mathbf{R}^{\mathrm{T}}\mathbf{H})| = |F(\mathbf{H})|$, that is all the reflections related to each other via $\mathbf{R}^{\mathrm{T}}\mathbf{H}=\mathbf{H}'$ have the same intensity. Such reflections are called ''**<u>equivalent</u>**''. It is trivial to prove that equivalent reflections have the same length, *i.e.* $|\mathbf{R}^{\mathrm{T}}\mathbf{H}|=|\mathbf{H}|$, and therefore share the same Bragg ϑ-angle! Hence, equivalent reflections contribute to the same Bragg peak, with the same intensity;

2) let us assume to have a $\mathbf{H}$ such that $\mathbf{H}= \mathbf{R}^{\mathrm{T}}\mathbf{H}$. In this case, equ.(26) leads to

$F(\mathbf{H}) = F(\mathbf{H}) \exp(-2\pi i\, \mathbf{H}\cdot\mathbf{t})$,

which requires that

- either $F(\mathbf{H}) = 0$ (***corresponding to the "<u>systematic extinction</u>"***),
- or $\exp(-2\pi i\, \mathbf{H}\cdot\mathbf{t}) = 1$, equivalent to having $\mathbf{H}\cdot\mathbf{t} =$ *integer*.

Let us see two examples.

A) Generic space group operation, with fractionary translation.

$$\bar{x} + \frac{1}{2}, y + \frac{1}{2}, \bar{z} + \frac{1}{4}$$

corresponding to:

$$\begin{pmatrix} \bar{1} & 0 & 0 \\ 0 & 1 & 0 \\ 0 & 0 & \bar{1} \end{pmatrix} \begin{pmatrix} \frac{1}{2} \\ \frac{1}{2} \\ \frac{1}{4} \end{pmatrix}$$

Its transpose coincides with the same matrix. Now, let us fix the invariant reflections:

$$\begin{pmatrix} \bar{1} & 0 & 0 \\ 0 & 1 & 0 \\ 0 & 0 & \bar{1} \end{pmatrix} \begin{pmatrix} h \\ k \\ l \end{pmatrix} = \begin{pmatrix} h \\ k \\ l \end{pmatrix} = \begin{pmatrix} \bar{h} \\ k \\ \bar{l} \end{pmatrix}$$

requiring that:
l=h=0
k=any.
Hence, reflections of the type:

$$\begin{pmatrix} 0 \\ k \\ 0 \end{pmatrix}$$

can be subjected to systematic extinction. Let us analyse the quantity:
0 * ½ +k* ½ +0 * ¼ = k/2;
if k/2≠integer, i.e. k=2n+1, then the reflection is extinct.

B) Centred lattice. I (*i.e.*: 1/2,1/2,1/2)
In the case of a centring (and here we focus on I, by way of example), systematic extinctions play a relevant role. In fact, centring cab be thought of as space group operation of the following type

$$\begin{pmatrix} 1 & 0 & 0 \\ 0 & 1 & 0 \\ 0 & 0 & 1 \end{pmatrix} \begin{pmatrix} 1/2 \\ 1/2 \\ 1/2 \end{pmatrix}$$

Therefore, *any* reflection is invariant with respect to $\mathbf{R}^T$! It ensues, reflections such that h/2 + k/2 +l/2 ≠integer must be extinct!!

Corrections

Now, let us see what corrections are required to account for some effects that affect observed diffraction intensities. Ideal diffraction intensities are expected to be
$I(\mathbf{H})_{ideal} = S\,|F(\mathbf{H})|^2$,
where S is a ''*scale*'' that accounts for the crystal size, incident intensity, detector efficiency and more. $I(\mathbf{H})_{ideal}$ must be corrected, and turned into $I(\mathbf{H})_{ideal\text{-}corrected}$, to take into account some effects that we discuss below, before being fully comparable with $I(\mathbf{H})_{experimental}$.

a) *Absorption*
X-ray passing through a solid undergo absorption according to the Beer-Lambert law, that is
$I(s) = I_0 \exp(-\mu \times s)$,
assuming "*s*" to be the distance travelled by radiation (path length). μ is the *attenuation coefficient* of a substance. All this is exemplified by the picture below:

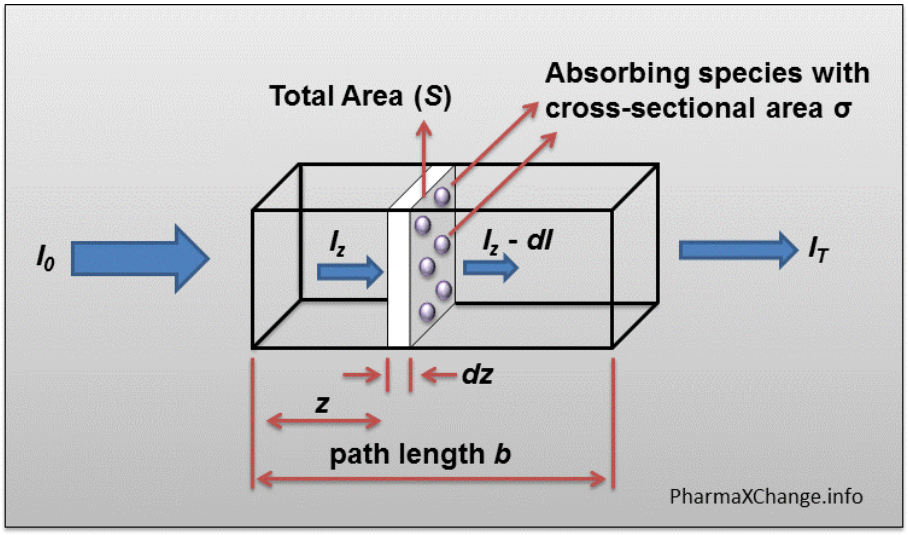

In general:

-μ depends on the direction of propagation of X-ray through a crystal. This is a natural consequence of anisotropy;

-μ is a function of the radiation energy, *i.e.* λ. Leaving aside any claim of precision, one can grossly state that

$\mu(\lambda) \propto \lambda^w$,

$w > 0$. Therefore, the higher the energy of a radiation, the less it is absorbed by the crystal. In the case of samples with highly anisotropic morphology, such as micas for instance, different diffraction processes follow paths having different lengths through the crystal. This makes it necessary to correct diffraction intensities as a function of the path through a crystal travelled by a specific diffracted beam. Such a correction is in general carried out during the "data reduction", *i.e.* that stage of treatment of the experimental intensities to turn them into a format ready to be processed by standard crystallographic programs.

b) **Primary and secondary extinction**

To be not confused with ''systematic extinction'', ''primary and secondary extinctions'' account for a loss in experimental diffraction intensity due to deviation from ideals of the crystal, and from limitations of the kinematic approach to diffraction that we have followed here.

Kinematic treatment of diffraction assumes that one has to deal with one incident beam and one diffracted beam, leaving the inter-correlations between beams aside. Dynamic theory of scattering is formulated to account for this aspect, too. We confine here our discussion of the subject within a few lines, but suffices it to know that primary extinction is often introduced starting from the general hypothesis that the phenomenon must be treated in terms of an exchange of energy between the incident and diffracted beams. Part of the incident beam turns into a diffracted signal and part undergoes bare absorption; the same takes place for diffracted beams, which suffer both absorption and re-entering the incident beam. In such a view, one can write down (Werner SA, 1974, Extinction in mosaic crystals, Journal of Applied Physics, **45**: 3246-3254)

$dJ_i = -\sigma_t J_i dx + \sigma J_d dx$

and

$dJ_d = -\sigma_t J_d ds + \sigma J_i ds$.

where *i* and *d* refer to incident and diffracted beam, *J* is the intensity, σ is the probability the beam to be diffracted/re-diffracted, whereas $\sigma_t = \sigma + \mu$; *x* and *s* refer to the coordinates along incident and diffracted beam, respectively. The physical meaning of the equations above is that energy is partly absorbed (μ), partly exchanged (σ) between the indent beam and the diffracted one. Naturally, we are restricting the discussion to one diffracted beam only. More complex treatments require the

introduction of many diffraction beams and, though theoretically valuable, they are difficult to be transposed into a practical use, at least within the reach of our interest.

After a few manipulations, one has the equations beneath

$$\frac{\partial J_i}{\partial x} = -\sigma_t J_i + \sigma J_d$$

$$\frac{\partial J_d}{\partial s} = -\sigma_t J_d + \sigma J_i$$

The equations above are restricted to the oversimplified case of two beams only: the incident beam and one diffracted signal; however, they allow one to achieve corrective expressions of practical usefulness. Their solution leads to the notion of ''extinction''. We distinguish further **primary** and **secondary** extinction: the *former*, if only one crystal is involved, the *latter*, if different ''blocks'', slightly misaligned one with respect to another, in a crystal contribute to the signal (*i.e.* mosaicism. In this case, one distinguishes between secondary extinction of type I, if the mosaic spread is dominant, and of type II, if the particle size is the most important aspect).
Practical correction is introduced according to the following scheme
$I(\mathbf{H})_{\text{ideal-corrected}} = I(\mathbf{H})_{\text{ideal}} / E_{hkl} = S\,|F(\mathbf{H})|^2 / E_{hkl}$,
where E_{hkl} is a coefficient that accounts for the reduction in intensity, and depends on the model used.

c) **Angle dependent corrections**
Further corrections are due to a combination of experimental geometry and physical effects. Let us consider two common cases:

1. Lorentz correction;
2. Polarization correction.

The first one is due to the actual volume size bathed by the X-ray and contributing to diffraction signals. For such a reason, it naturally depends on the *experimental geometry* one uses to collect data. A common expression taking into account the Lorentz effect on intensity is

$$I(\mathbf{H})_{ideal-corrected} = \frac{I(\mathbf{H})_{ideal}}{\sin(2\vartheta)}$$

The second case accounts for the fact that the incident X-ray beam is composed of two vectors, normal to one another, providing vertical and horizontal polarizations. Assuming an incident beam with intensity equally distributed over horizontal and vertical components, then the correction is:

$$I(\mathbf{H})_{ideal-corrected} = \frac{1+\cos(2\vartheta)^2}{2} I(\mathbf{H})_{ideal}$$

In full, the Lorentz-polarization correction, in a very ''popular'' form, results in

$$I(\mathbf{H})_{ideal-corrected} = \frac{1+\cos(2\theta)^2}{\sin(2\theta)} I(\mathbf{H})_{ideal}\,.$$

Note that such correction has to be always considered taking into account the experimental setup used for the experiment (collection geometry, polarization filters, etc..).

Altogether, one can write

$$I(\mathbf{H})_{ideal-corrected} = \frac{1+\cos(2\theta)^2}{\sin(2\theta)} \left|F(\mathbf{H})\right|^2 \times S \times \frac{1}{E(\mathbf{H})} \times (\textbf{absorption correction}) \qquad (27)$$

XIV. SINGLE CRYSTAL DIFFRACTION EXPERIMENTS

Experimental targets
Let us consider a ‘’canonical’’ single crystal X-ray diffraction experiment.

In general, such an experiment is organised as follows:
1) **diffraction intensities collection**. A crystal is positioned on a special holder and mounted on a capillary in a ‘’single crystal diffractometer’’. Such an instrument allows one to orient a crystal by means of rotations around four axes (classical Eulerian geometry and K-geometry). More geometries are available, but they are here skipped for the sake of simplicity. It suffices to keep in mind that such collection geometries depend on the detecting method used. For instance: i) classic scintillator, measuring one reflection a time, or ii) area detector, such as an imaging plate or a charge-coupled-device, both collecting many intensities a time, so that any orientation can be achieved and any diffraction intensity can in principle be measured, insofar as the experimental wavelength used makes accessible the related portion of the reciprocal lattice. In so doing, the experimenter obtains a set of
$hkl \quad I_{exp} \quad \sigma(I)$
records. For each diffraction process, its *hkl*, intensity and uncertainty are recorded.
2) **data reduction**. Once the ‘’raw’’ intensities have been measured, one has to correct them for the effects we have mentioned above (angular correction and absorption). In general, physical extinction is accounted for during the ‘’structure refinement’’ stage.
3) data elaboration. We face two possible common strategies:
(**A**) structure solution. In this case, one does not know almost anything about the structure, *i.e*. atomic arrangement in the crystal under study. Therefore, one’s goal is to determine the atomic positions, at least at a first level of approximation. There exist techniques, which allow one to solve structures. We mention here: (1) direct methods, (2) maximum entropy and (3) charge flipping. The gist of such methods consist in determining atoms’ positions by means of the electron density that is indirectly inferred, *via* particular theoretical techniques, from the experimental intensities.

Direct methods
They have been extensively developed in the last fifty years and have achieved a high level of “maturity” today (Direct Methods, C. Giacovazzo, Academic Press, 1980). A vast theoretical bulk of knowledge has been consolidated and it would be beyond the aims of the present course to present it. Let us just say that most of the effort is directed to somehow determine the “phases” of the reflections, whose intensities are collected by experiments. We focus on one particular case, known as “Sayre equation”. Let us write (for the sake of simplicity we suppose that $F_{\mathbf{H}}$ has been defined in such a way that its Fourier transform provides a direct link to electron density with proportion coefficient equal to 1)

$$\rho(\boldsymbol{x}) \times \rho(\boldsymbol{x}) = \sum_{\mathbf{H},\mathbf{L}} F_{\mathbf{H}} e^{2\pi i \boldsymbol{x}\mathbf{H}} F_{\mathbf{L}} e^{2\pi i \boldsymbol{x}\mathbf{L}} = \sum_{\mathbf{H},\mathbf{L}} F_{\mathbf{H}} F_{\mathbf{L}} e^{2\pi i \boldsymbol{x}(\mathbf{H}+\mathbf{L})} = \sum_{\mathbf{H},\mathbf{M}} F_{\mathbf{H}} F_{\mathbf{M}-\mathbf{H}} e^{2\pi i \boldsymbol{x}\mathbf{M}} = \sum_{\mathbf{M}} F_{\mathbf{M}}^{sq} e^{2\pi i \boldsymbol{x}\mathbf{M}}$$

and from the equation above it descends that

$$F_{\mathbf{M}}^{sq} = \sum_{\mathbf{H}} F_{\mathbf{H}} F_{\mathbf{M}-\mathbf{H}}$$

which provides a very useful relationship that correlates structure factors of electron density with those of its square. Let us make a further approximation, that is

$$F_{\mathbf{M}}^{sq} \approx \sum_{=1,atoms} f_j^{sq} e^{2\pi i \mathbf{M}\boldsymbol{x}_j} \approx \sum_{=1,atoms} f_j^2 e^{2\pi i \mathbf{M}\boldsymbol{x}_j}$$

Let <*f*> be the average over the atomic scattering powers, *i.e.* f_j. Then, assuming

$$\frac{< f_j >}{< f >} \approx 1 + \sigma$$

we can set

$$\frac{1}{<f>} F_{\mathbf{M}}^{sq} = \frac{1}{<f>} \sum_{=1,atoms} f_j^2 e^{2\pi i \mathbf{M} \boldsymbol{x}_j} = \sum_{=1,atoms} (1 + \sigma_j) f_j e^{2\pi i \mathbf{M} \boldsymbol{x}_j} \approx \sum_{=1,atoms} f_j e^{2\pi i \mathbf{M} \boldsymbol{x}_j} = F_{\mathbf{M}}$$

and therefore

$$F_{\mathbf{M}} = \frac{1}{<f>} \sum_{\mathbf{H}} F_{\mathbf{H}} F_{\mathbf{M}-\mathbf{H}}.$$

Introducing a polar representation, we can write

$$|F_{\mathbf{M}}| e^{i\theta_{\mathbf{M}}} = \frac{1}{< f >} \sum_{\mathbf{H}} |F_{\mathbf{H}} F_{\mathbf{M}-\mathbf{H}}| \, e^{i\theta_{\mathbf{H}}} e^{i\theta_{\mathbf{M}-\mathbf{H}}}.$$

If in the summation above one term is significantly larger than the others, then we expect that

$$|F_{\mathbf{M}}| \approx \frac{1}{< f >} |F_{\mathbf{H}} F_{\mathbf{M}-\mathbf{H}}|$$

and, in particular,

$$e^{i\vartheta_{\mathbf{M}}} \approx e^{i\theta_{\mathbf{H}}} e^{i\theta_{\mathbf{M}-\mathbf{H}}}$$

i.e.

$$\theta_{\mathbf{M}} \approx \theta_{\mathbf{H}} + \theta_{\mathbf{M}-\mathbf{H}}.$$

Moreover, note that

$$e^{i\theta_{\mathbf{M}}} = \frac{\sum_{\mathbf{H}} |F_{\mathbf{H}} F_{\mathbf{M}-\mathbf{H}}| \, e^{i\theta_{\mathbf{H}}} e^{i\theta_{\mathbf{M}-\mathbf{H}}}}{|\sum_{\mathbf{H}} |F_{\mathbf{H}} F_{\mathbf{M}-\mathbf{H}}| \, e^{i\theta_{\mathbf{H}}} e^{i\theta_{\mathbf{M}-\mathbf{H}}}|}$$

and it follows

$$\tan(\theta_{\mathbf{M}}) = \frac{\sum_{\mathbf{H}} |F_{\mathbf{H}} F_{\mathbf{M}-\mathbf{H}}| \sin(\theta_{\mathbf{H}} + \theta_{\mathbf{M}-\mathbf{H}})}{\sum_{\mathbf{H}} |F_{\mathbf{H}} F_{\mathbf{M}-\mathbf{H}}| \cos(\theta_{\mathbf{H}} + \theta_{\mathbf{M}-\mathbf{H}})}.$$

Note that, if one can reliably replace f_j with <*f*>, then the equation above changes into

$$\tan(\theta_{\mathbf{M}}) \approx \frac{\sum_{\mathbf{H}} |E_{\mathbf{H}} E_{\mathbf{M}-\mathbf{H}}| \sin(\theta_{\mathbf{H}} + \theta_{\mathbf{M}-\mathbf{H}})}{\sum_{\mathbf{H}} |E_{\mathbf{H}} E_{\mathbf{M}-\mathbf{H}}| \cos(\theta_{\mathbf{H}} + \theta_{\mathbf{M}-\mathbf{H}})}$$

where we have introduced

$$E_{\mathbf{H}} = \sum_{=1,atoms} e^{2\pi i \mathbf{H} \boldsymbol{x}_j}.$$

Another important aspect, relevant to the "direct methods", is the one that relates the invariance on translation of the product of a set of structure factors to their phases. Let us have, for instance,

$$F_{\mathbf{H}} F_{\mathbf{H}'} F_{\mathbf{H}''}$$

and seek the required conditions for the product to be left unchanged by a translation of the origin. A translation of the origin, $\boldsymbol{t}_O$, affects a structure factors in terms of a phase, *i.e.*

$$e^{2\pi i \boldsymbol{t}_O \mathbf{H}}$$

which thing implies that the invariance requirement is provided by
$e^{2\pi i \boldsymbol{t}_O(\mathbf{H}+\mathbf{H}'+\mathbf{H}'')}$,
leading to

$$\mathbf{H} + \mathbf{H}' + \mathbf{H}'' = 0$$

if $\boldsymbol{t}_O$ is supposed to be a *fully general* translation. Less restrictive conditions are called if $\boldsymbol{t}_O$ assumes specific values.
Another condition is provided by a more general invariance requirement, that is the product be an absolute invariant, *i.e.*
$F_{\mathbf{H}}F_{\mathbf{H}'}F_{\mathbf{H}''} = |F_{\mathbf{H}}F_{\mathbf{H}'}F_{\mathbf{H}''}|e^{2\pi i(\theta_{\mathbf{H}}+\theta_{\mathbf{H}'}+\theta_{\mathbf{H}''})}$
from which it descends

$$\theta_{\mathbf{H}} + \theta_{\mathbf{H}'} + \theta_{\mathbf{H}''} = integer.$$

Maximum Entropy Method
Maximum Entropy Method (MEM) was introduced in crystallography by Collins (D. M. Collins, 1982, Electron density images from imperfect data by iterative entropy maximization, Nature Vol. 298 p.49), from information theory (E. T. Jaynes, 1957, Information theory and statistical mechanics, Phys. Rev. Vol.106, p.620). The general principle is as follows.
Let us "pixelize" the elementary cell's electron density, so that each j-pixel, corresponding to a small volume (voxel), is equivalent to a region in which $\rho(\boldsymbol{r})$ has the average value of ρ_j. Any ρ_j, in turn, is expressed like the total number of electrons in the elementary cell (N_e) by p_j, *i.e.* the probability to have electrons in the j^{th}-voxel. The problem of determining the electron density is changed therefore into the problem of determining a probability distribution.
Among the possible probability distributions, we choose "the least committal" one, that is the distribution least affected by the initial choice of the experimenter, on the one hand, and such that it is able to correctly reproduce the measured diffraction intensities, on the other hand. This combination of requirements is achieved by looking for the $\{p\}$ distribution that maximises the following entropy functional

$$S = -\sum_{j=1,Npixels} p_j \ln(p_j)$$

under the constraint that

$$\sum_{j=1,Npixels} p_j = 1.$$

The electron density is derived accordingly, *i.e.*
$\rho_j = p_j \times N_{electrons}$
where $\rho(\boldsymbol{x})$ has been approximated by a grid, each node corresponding to a pixel.

Charge flipping
This method has gained large popularity in the last years, owing to its simplicity and efficacy.
Let us assume to have a set of observed reflections, $\{|F(\mathbf{H}_j)_{obs}|\}=\{|F_{j,obs}|; \mathbf{H}_j \in \mathbf{M}$, for simplicity $j \in \mathbf{M}\}$, and a discrete electron density function ρ^{old}, consistent with the chemical composition of the compound under study, and having Fourier coefficients $\{F^{old}_l\}$.
We generate a new set of structure factors applying the following algorithm:

$$F_j^{new} = \frac{F_j^{old}}{\left|F_j^{old}\right|} \left|F_{j,obs}\right|$$

if j belongs to **M**, and

$$F_k^{new} = F_k^{old}$$

if *k* does not belong to **M**.
From $\{F^{old}{}_I\}$ we calculate a new electron density, ρ^{new}, setting possible further restraints in terms of absolute value to reduce numerical noise on individual pixel, such as $\rho^{new}{}_m = 0$ if $\rho^{new}{}_m <$ limit value. The algorithm proceeds until achievement of a convergence on the electron density function that does not change significantly with respect to the previous cycle.

(**B**) structure refinement. In this case, one knows the structure, and the attention points to discover details (such as the cation partitioning, *i.e*. the occupancies) or to understand the response under external perturbations, like pressure and/or temperature. Let us see now the fundamentals of structure refinement.
Structure refinement
The general idea is to change structure parameters to fit experimental intensities collected by a single crystal diffractometer. In this light, the strategy aims at modifying a structure model to reproduce as precisely as possible the observations. Let us assume:
$I(\mathbf{H},\{\omega\})_{\text{ideal-corrected}}$= intensity associated with **H**;
{ω}= set of parameters related to atomic positions, displacement parameters, occupancies and extinction coefficients.
We minimize the following quantity
$$\chi^2 = \frac{1}{N-M}\sum_H \left[I(\mathbf{H},\{\omega\})_{ideal-corrected} - I(\mathbf{H})_{experimental}\right]^2/\sigma(\mathbf{H})^2$$
where N is the number of observed intensities and M corresponds to the degrees of freedom, *i.e*. {ω}. Therefore, the {ω}-values are changed until the minimum of χ^2 is achieved. This way, one can determine how structure parameters, *i.e*. {ω}, change upon pressure and/or temperature, or, in general, one is able to explore the structure details of a crystal. Naturally, one must know at a first level of precision the structure of the mineral under study.

XV. POWDER DIFFRACTION

Powder diffraction: general aspects
What happens if one uses powders, instead of single crystals? Let us assume that the crystals of a powder be randomly oriented. An X-ray beam impinging a powder meets therefore crystals so disposed as to concur to any diffraction process compatible with the Bragg law. Given the relationship
$2\, d_{hkl} \sin(\vartheta)=\lambda$,
which is fulfilled by all the momentum transfer vectors such as
$|Q|=|h\,\mathbf{a^*} + k\,\mathbf{b^*} + l\,\mathbf{c^*}|=1/\,d_{hkl}$,
then one concludes that ‘’many’’ crystals will be able to satisfy the equation above, and give contribution to the signal appearing at 2ϑ. Naturally, all the diffraction processes sharing the same |**Q**| contribute to the same 2ϑ-peak.

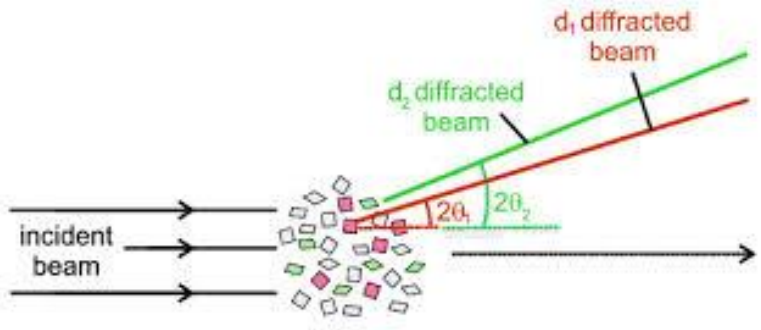

Two main experimental geometries can be considered:

1) **Reflection geometry** (parafocussing geometry), implemented by a Bragg-Brentano diffractometer, as displayed below

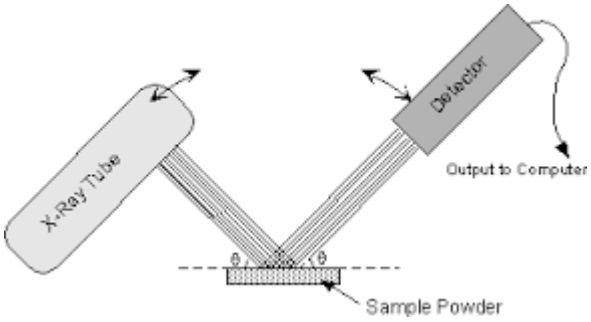

and giving an output like

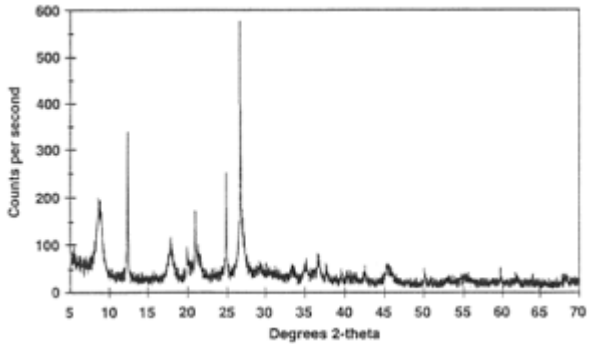

2) **Transmission geometry**, for instance a Debye-Scherrer set-up, as reported beneath

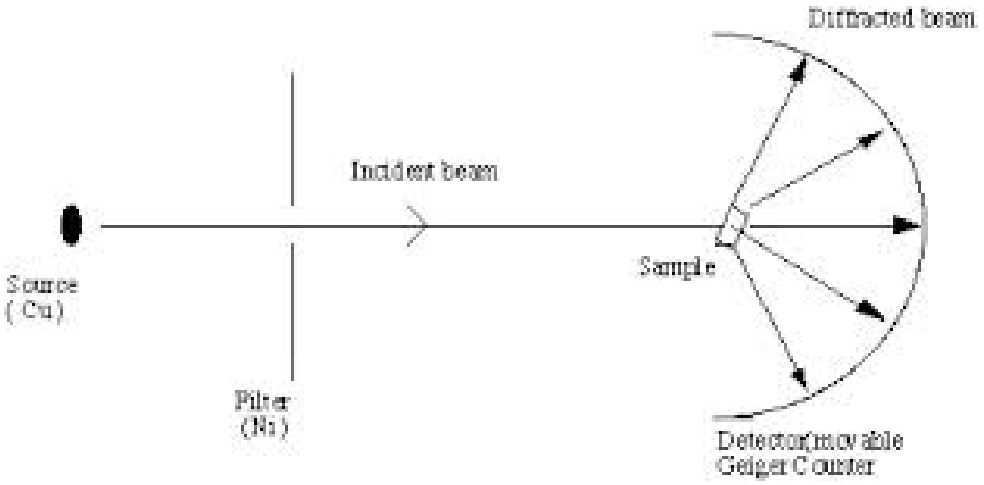

and leading to an output of the type

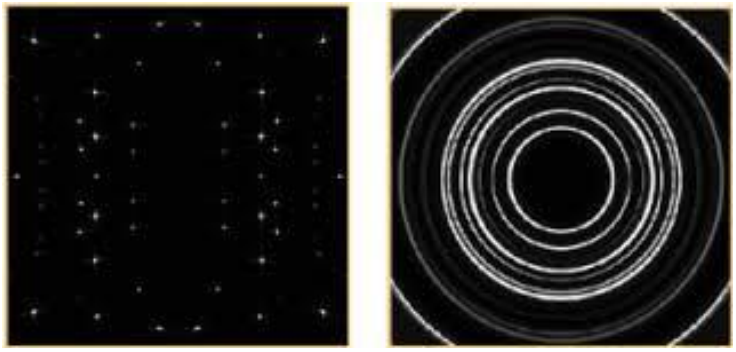

Note that the *diffraction rings* above can be turned into standard diffraction patterns (*i.e.* 2ϑ-Intensity) by 2D-integration.

Goals of powder diffraction

One has at one's reach several possible goals by powder diffraction:
1) **phase composition determination**. Every crystal phase has a specific powder diffraction pattern, characterized by the location of the peaks and their intensities. This way, the powder diffraction pattern of a phase somewhat represents a sort of ''fingerprints'' of the phase itself. In case of a mixture, powder diffraction is the appropriate technique to determine the occurring phases and quantify them. In fact, each phase contributes to the total diffraction profile with its own pattern that participates proportionally to the amount of the phase in question. The positions of the peaks and their relative intensities allow recognition of the occurring phases, in terms of those best matching the ones contained in powder diffraction databases. Such databases collect the powder diffraction patterns of all hitherto investigated crystal substances of a given class of materials (for instance: *minerals*). Moreover, it is possible to determine also the relative occurrence of a given phase, in terms of its percentage by weight. Such an aspect renders powder diffraction analysis an extremely powerful tool for industrial applications. We shall discuss this aspect in the section below devoted to the ''Rietveld method''.
2) **lattice parameters measurement**. As discussed in XII(Braw law), it is straightforward to extract lattice parameters from a powder diffraction pattern. Each peak allows one to relate its position to a given d_{hkl}, which in turn depends on the **G*** matrix, *i.e.* the *inverse* of **G**, whose terms are trivial functions of a, b, c, α, β, γ.
3) **structure refinement and solution**. Although single crystal diffraction represents the best way to investigate the structure of a crystal phase, yet powder diffraction allows one to carry out structure refinements by the Rietveld method. Advanced techniques of powder diffraction analysis make it possible even to solve structures. The use of powder diffraction for structure investigations is necessary when no appropriate single crystals are available.
4) **micro-structure analysis**. The analysis of the powder diffraction profile allows one to infer pieces of information on micro-strain, crystallite size and texture. In particular, micro-strain and coherence domain size are related to the peak's **broadening**, *i.e.*

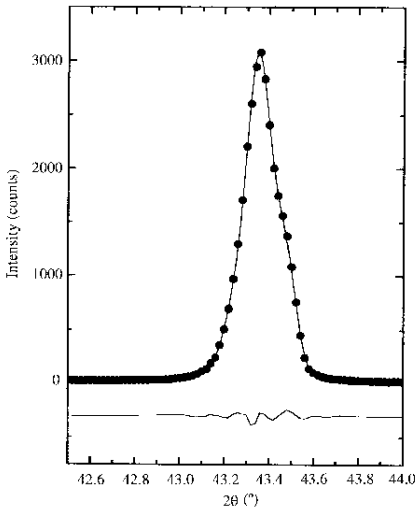

whereas texture depends on the tendency of crystals to take preferred orientations favouring diffraction processes that ''feed'' particular peaks.

The Rietveld method

Now we discuss the Rietveld method that has achieved much popularity as a technique to extract information from processing powder diffraction patterns. The fundamentals are reported in the paper by Rietveld, published with the ''Journal of Applied Crystallography'', 1969, **2**: 65-71. The general idea consists in making a theoretical diffraction pattern match the observed one by changing the parameters related to the mineral's structure.
Let us analyse what happens around a given peak, *hkl*. By the way, do not forget that all diffraction signals sharing the same $|\mathbf{Q}_{hkl}|$ contribute to the intensity of the same peak.

The intensity of powder diffraction at 2ϑ is modelled in terms of

$$I(2\vartheta)_{\text{theo}} = \textit{background}(2\vartheta) + S \times M_{hkl} \times C(2\vartheta)_{hkl} \times |F_{\text{hkl}}|2 \times \text{profile}(2\vartheta) \qquad (28)$$

where:
background(2ϑ)=it is the background function, accounting for all spurious contribution to scattering such as the detector noise, incoherent scattering (*i.e.* not related to diffraction) and many more. In principle, it should be more or less ''flat'', but in practice it can result in a structured contribution, in particular if conditioning devices are on, or if angle-dependent fluorescence phenomena take place. Anyway, it *does not* contribute to the Bragg peak and acts somewhat as a ''baseline''.
S=it is the *scale* that accounts for all those effects affecting intensity such as the amount of sample, efficiency of detecting, incident beam intensity, etc
M_{hkl} =molteplicity of *hkl*. It accounts for all the *equivalent* reflections (see XIII. Systematic extinction) contributing to the same peak and having equal intensities.
$C(2\vartheta)_{hkl}$ =it is a generic angle dependent correction factor. It accounts for absorption, extinction preferred orientation and geometric corrections. It is a very complex quantity, which turns out to be as a function of the experimental setup and geometry.
$|F_{\text{hkl}}|^2$=it controls the ''height'' of a peak.
profile(2ϑ)=it describes the ''shape'' of a peak. Naturally. Such a function is centred around each peak, whose position if determined by the Bragg law and the cell parameters. In this view, the experimental profile is modelled by summing all the theoretical patterns due to every peak.

The most general profile function is a folding between
a ***sample function***, $S(2\vartheta)$
and
an ***instrument function*** $F(2\vartheta)$,
the former accounting for all that is due to a specimen, the latter for the instrument contribution; in short

$$P(2\vartheta) = F(2\vartheta)^* S(2\vartheta) = \int_{-\infty}^{\infty} F(2\vartheta')S(2\vartheta - 2\vartheta')d(2\vartheta') \quad (29)$$

In practice, we show some common profile functions to model peaks below:

- *G*aussian$(2\vartheta) \propto 1/(\sigma\sqrt{2\pi})\exp[-(2\vartheta\text{-}2\vartheta_{hkl})^2/2\sigma^2]$
- *L*orenzian$(2\vartheta) \propto \gamma/[\pi(2\vartheta\text{-}2\vartheta_{hkl})^2+\gamma^2]$
- *V*oigt$(2\vartheta) \propto G(2\vartheta)^*L(2\vartheta)=\int_{-\infty}^{\infty} G(x')L(x-x')dx'$ $x=2\vartheta$
- *P*seudo-*V*oigt$(2\vartheta) \propto \eta\times G(2\vartheta)+(1\text{-}\eta)\times L(2\vartheta)$

The choice of a profile function depends on the experimental setup (instrument geometry, radiation and source).
By means of the profile analysis of diffraction pattern, one is able to extract pieces of information related to **strain** and **coherence domain size** of the sample under study. Strain represents the ''deviation from the ideals'' of a perfect crystal structure. Intuitively, the larger a peak, the more the sample diverts from a perfect structure.
A simple way to define a relationship between <u>strain</u> and scattering angle is the following one:
let us take d for a d-spacing and Δd for the deviation from its ideals. Then the strain is defined by

$\Delta d/d = \varepsilon_s = [\lambda\times \cos(\vartheta)\times\Delta\vartheta/(2\sin(\vartheta)^2)]/[\,[\lambda/(2\sin(\vartheta))]=\mathrm{ctg}(\vartheta)\times\Delta\vartheta$
and therefore
$\Delta\vartheta = \varepsilon_s\times\mathrm{tg}(\vartheta)$. (30.a)

Such a relationship offers a first-approximation way to rationalise how peak broadening depends on strain. We do not discuss further this topic, which has been subject of many investigations and developments.
<u>Coherence domain size</u> gives an idea about how large the crystal regions that behave like coherent structure (*i.e*. more or less like ''crystals'') are. In this view, one can assume that a measure of such a feature is provided by the ''size'' of each reciprocal lattice node, which in principle should be a perfect and dimensionless geometric point in perfect crystal. Therefore
$\Delta d^* = \varepsilon_d = \Delta d/d^2 = 2\times\cos(\vartheta)\times\Delta\vartheta/\lambda$,
and therefore
$\Delta\vartheta = \varepsilon_d/(2\times\lambda\times\cos(\vartheta))$. (30.b)

Quantitative phase analysis (QPA)

One of the most important ability of the Rietveld method is that it allows one to determine the relative amounts of the crystal phases constituting a mixture. Starting from Equ. (16.e), one assumes to have a powder constituted by phases (α), each with many crystals (j). Then, the contribution of the α-phase to **H** is

$I(H)_\alpha = \sum_j I(\mathbf{H})_{\alpha,j} \propto \sum_j \psi(j,\mathbf{H})_\alpha \times V_{j-crystal,\alpha}/V_\alpha^2 \times |F(\mathbf{H})_\alpha|^2$,
where $\psi(j,\mathbf{H})_\alpha$ measures the probability that the jth crystal be so oriented as to contribute to the **H**-diffraction. One assumes that $\varsigma(j,\mathbf{H})_\alpha$ depends mainly on **H**; therefore

$I(\mathbf{H})_\alpha \propto \varsigma(\mathbf{H})_\alpha \times \sum_j V_{j\text{-crystal},\alpha}/V_\alpha^2 \times |F(\mathbf{H})_\alpha|^2$.
If one then takes that the crystal volumes are very similar, then one attains

$I(\mathbf{H})_\alpha \propto \varsigma(\mathbf{H})_\alpha \times V_{total,\alpha}/V_\alpha^2 \times |F(\mathbf{H})_\alpha|^2$

where $\varsigma(\mathbf{H})_\alpha$ accounts for by the preferred orientation, and it can be modeled in very efficient ways. $V_{total,\alpha}$ is expressed through the ratio "phase's weight in mixture/phase's density". If:

M=total mass of powder
ω_α=percentage of the α-phase;
ρ_α=density of the α-phase,

then, the contribution to of the α^{th} phase to **H** is
$I(\mathbf{H})_\alpha \propto \varsigma(\mathbf{H})_\alpha \times M \times \omega_\alpha/\rho_\alpha \times |F(\mathbf{H})_\alpha|^2 / V_\alpha^2$. (31)

This way, one recognizes that by the ω–term it is possible to account for the content of a given phase. Naturally, ω can be determined by the least-square method, searching the best matching between theoretical and observed powder diffraction patterns, if it is assumed that the structures of the involved phases are known.

Rietveld refinement

The general principle is to change a set of parameters (structure parameters: coordinates, occupancy factors and thermal factors; lattice parameters; preferred orientation coefficients; absorption coefficients; phase-content; strain and coherence domain size coefficients; possible experimental parameters; background function parameters) so that the theoretical profile nears as much as possible the observed one. Hence, one aims to minimize the following target

$\chi^2 = \sum_j (I(2\vartheta_j)_{theoretical} - I(2\vartheta_j)_{observed})^2/\sigma(j)^2$ (32)

where $2\vartheta_j$ is a point of the diffraction pattern, and $/\sigma(j)$ is the uncertainty associated to the intensity at that point. The $I(2\vartheta_j)_{theoretical}$ can be modelled as we have discussed above, and it depends therefore on many parameters that are adjusted so that the theoretical profile matches the experimental one. In doing so, one can extract many pieces of information: crystal structure, deviation from ideals, texture and phase composition.

XVI. NON-CRYSTAL SYSTEMS

Now, let us see how to deal with a non-crystal structure (suggested reading: Underneath the Bragg peaks: structural analysis of complex materials, T Egami and SJL Billige, Pergamon Materials Series, Ed. R.W.Cahn, 2003). Let us start from the general notion that the X-ray scattered intensity of a ''cluster'' of atoms without any translation invariance is governed by the general equation:

$I(\mathbf{Q})_{obs} \propto \Im(\mathbf{Q}) = |\int e^{i\mathbf{Q}\cdot\mathbf{r}} \rho(\mathbf{r}) d\mathbf{r}|^2 = |\sum f(\mathbf{Q})_j \times e^{-i\mathbf{Q}\cdot\mathbf{R}_j}|^2$ (33)

where j spans over the atoms. Note that in total scattering formalism one uses a redefinition of the momentum transfer vector in terms of $\mathbf{Q}=2\pi/\lambda\times(\mathbf{K}_f-\mathbf{K}_i)$. Equ.(33) can be cast into

$$\Im(\mathbf{Q})=\int e^{i\boldsymbol{Q}\cdot\boldsymbol{r}}\rho(\boldsymbol{r})d\boldsymbol{r}\times\int e^{-i\boldsymbol{Q}\cdot\boldsymbol{r}'}\rho(\boldsymbol{r}')d\boldsymbol{r}'=\int e^{i\boldsymbol{Q}\cdot(\boldsymbol{r}-\boldsymbol{r}')}\rho(\boldsymbol{r})\rho(\boldsymbol{r}')d\boldsymbol{r}\,d\boldsymbol{r}' \quad (34.a)$$

One takes then

$$P(\mathbf{R})=(1/2\pi)^3\int\Im(\mathbf{Q})\times e^{-i\mathbf{Q}\cdot\mathbf{R}}\,d\mathbf{Q} \quad (34.b)$$

which, combined with (34.a), leads to

$$P(\mathbf{R})=(1/2\pi)^3\int e^{i\boldsymbol{Q}\cdot(\boldsymbol{r}-\boldsymbol{r}')}\times e^{-i\boldsymbol{Q}\cdot\boldsymbol{R}}\rho(\boldsymbol{r})\rho(\boldsymbol{r}')d\boldsymbol{r}\,d\boldsymbol{r}'\,d\mathbf{Q}=$$

$$\int\delta(\boldsymbol{r}-\boldsymbol{r}'-\boldsymbol{R})\rho(\boldsymbol{r})\rho(\boldsymbol{r}')d\boldsymbol{r}\,d\boldsymbol{r}'=\int\rho(\boldsymbol{r}'+\boldsymbol{R})\rho(\boldsymbol{r}')d\boldsymbol{r}' \quad (35)$$

Equ.(35) is similar to (25), given that here, too, $P(\mathbf{R})$ has maxima for **R** corresponding to inter-atomic vectors. This is a general properties for any function that can be expressed by equ.(33).

In the case of amorphous materials, one may safely assume that $\Im(\mathbf{Q})$ and $P(\mathbf{R})$ be **isotropic**, *i.e.* they depend on $|\mathbf{Q}|=Q$ and $|\mathbf{R}|=R$. Therefore, eq.(34.b) turns into

$$P(R)=(1/2\pi)^3\times\int\Im(Q)\times e^{-iQ\cdot R\cdot\cos(\varphi)}\,Q^2\sin(\varphi)dQd\varphi\,d\theta \quad (36)$$

where $\theta:[0,2\pi]$, $\varphi:[0,\pi]$; all this leads to

$$P(R)=1/(2\pi^2R)\times\int\Im(Q)\times[\sin(Q\cdot R)/Q]\times Q^2\,dQ\,. \quad (37)$$

Equ.(37) is troublesome for integration, and in practice a different approach is followed to tackle total scattering from non-crystalline solids.

Let us re-start from

$$I(\mathbf{Q})_{obs}\propto$$

$$1/N\sum_j f(Q)_j e^{i\mathbf{Q}\cdot\mathbf{Rj}}\sum_k f(Q)_k e^{-i\mathbf{Q}\cdot\mathbf{Rk}}=1/N\sum_j f(Q)_j{}^2+1/N\sum_{k,j\atop k\neq j} f(Q)_k f(Q)_j e^{i\mathbf{Q}\cdot(\mathbf{Rj}-\mathbf{Rk})} \quad (38)$$

where N is the number of atoms. If we put

$$\langle f(Q)^2\rangle=1/N\sum_j f(Q)_j{}^2$$

then one has

$$I(\mathbf{Q})_{obs}\propto\langle f(Q)^2\rangle\times[1+1/N\sum_{k,j\atop k\neq j}(f(Q)_k f(Q)_j)/\langle f(Q)^2\rangle\times e^{i\mathbf{Q}\cdot(\mathbf{Rj}-\mathbf{Rk})}] \quad (39.a)$$

and

$$I(\mathbf{Q})_{obs}\propto\langle f(Q)^2\rangle\times S(\mathbf{Q}). \quad (39.b)$$

Note that $S(\mathbf{Q})=1$ corresponds to an array of equal scatterers, as $\langle e^{i\mathbf{Q}\cdot\mathbf{R}}\rangle=0$ in equ.(39.a). Note that $\lim_{\mathbf{Q}\to0,N\to\infty}S(\mathbf{Q})=1$.

In equ.(39.b), we introduce the notion of the **total scattering structure function**, $S(\mathbf{Q})$, wherefrom one has

$$I(\mathbf{Q})_{obs,normalised}=I(\mathbf{Q})_{obs}/\langle f(Q)^2\rangle\propto S(\mathbf{Q})=\left|\int e^{i\boldsymbol{Q}\cdot\boldsymbol{r}}\rho_A(\boldsymbol{r})d\boldsymbol{r}\right|^2 \quad (40)$$

$\rho_A(\mathbf{r})$ is somewhat of a ''normalized electron density'' ($\int \rho_A(\boldsymbol{r})d\boldsymbol{r} \approx 1$; for an array of perfectly equal scatterers then $\rho_A(\boldsymbol{r}) = \rho_0 = 1/V$) and naturally one can introduce

$P_A(\mathbf{R}) = (1/2\pi)^3 \times \int S(\mathbf{Q}) \times e^{-i\mathbf{Q}\cdot\mathbf{R}}\, d\mathbf{Q}$

that preserves the properties already discussed for equ. (35). It is usual, then, to subtract 1 from $S(\mathbf{Q})$, so as to retain the part dependent on couples of *different* atoms (in other terms, it can be likened to subtracting a distribution of perfectly equal scatterers from the actual one), and recast the equation above in the following shape

$$[g(R)-1]\times\rho_0 = (1/2\pi^2 R)\times\int [S(Q)-1]\times[\sin(Q\cdot R)/Q]\times Q^2 dQ. \quad (41)$$

$g(R)$ is the ***pair distribution function***, and its maxima correspond to inter-atomic distances. ρ_0, as stated above, is the normalized scatterer's uniform density, $1/V$. Given that the argument of g is a distance, R, then one commonly uses the term ***radial distribution function***. Note that it is possible to define $S_{\alpha\beta}(Q)$, where α and β fix chemical species; we skip here for the sake of simplicity such a further notion.

By way of example, it is shown underneath a classic trend exhibited by $g(R)$

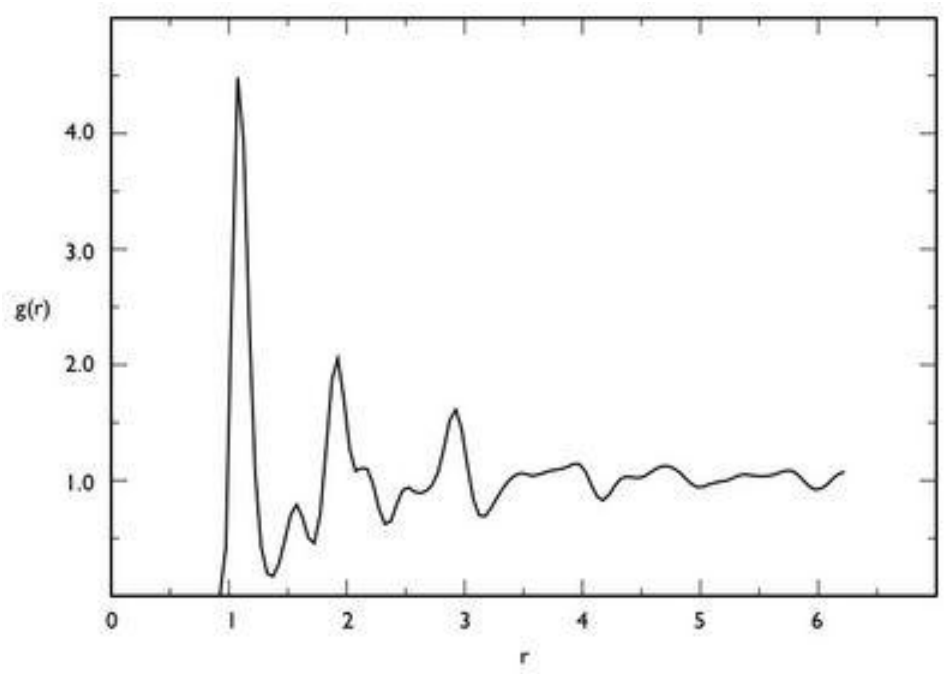

The positions of peaks allow one to determine interatomic distances, corresponding to an atomic couple.

DIFFRACTION EXPERIMENTS

XVII. DETECTORS

Detectors allow one to record scattered X-ray, neutrons or electrons, and their collection geometry affect the whole design of the instrument. Leaving aside the case of electrons, we focus here on how to detect X-ray or neutrons.

We discriminate between *point-detectors* (**PD**) and *area-detectors*, or *position-sensitive-detectors* (**PSD**). The former allow one to record radiation over a narrow space interval, from which one says them ‘’*point*’’ devices. Such a recording architecture is off-date, and we discuss it here for the sake of completeness and for making readers better understand the natural development of the instrumentations for diffraction. The latter, conversely, enable data recording of many diffraction signals at a time, and have a 2D-recording geometry.

Single crystal

PDs record peak profiles by exploring a single diffraction signal through a rocking of sample/detector around the related *hkl*-momentum, obtaining what shown below:

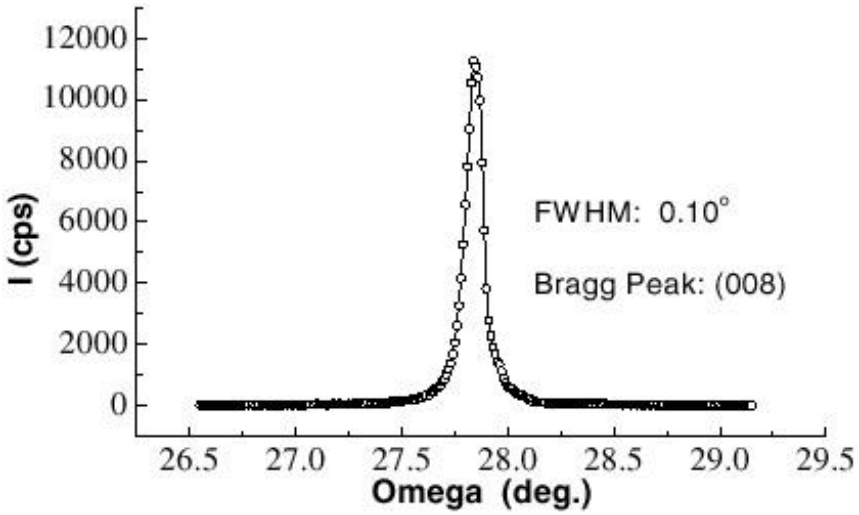

The area of the peak corresponds to the ‘’observed intensity’’ of *hkl*. At each position of the rocking-movement, corresponding to a given angular value, the detector measures the diffracted photons. This explains why the profile is constituted by many ‘’points’’, each one being a recording at a given rocking angle.

In the case of **PSD**, one records ‘’spots’’ that occur where a diffraction beam strikes the detector’s surface, giving rise to recording images like those below, wherein each spot represents the ‘’intersection’’ of a diffracted beam with the detector surface.

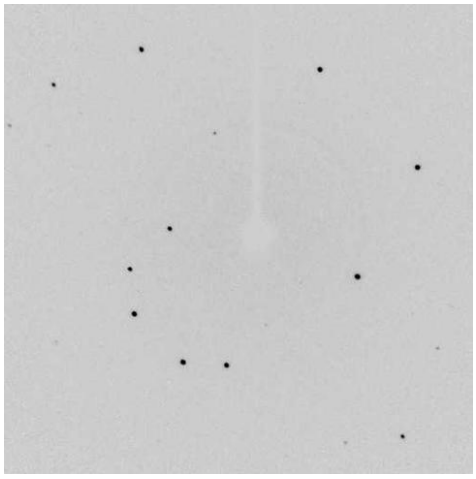

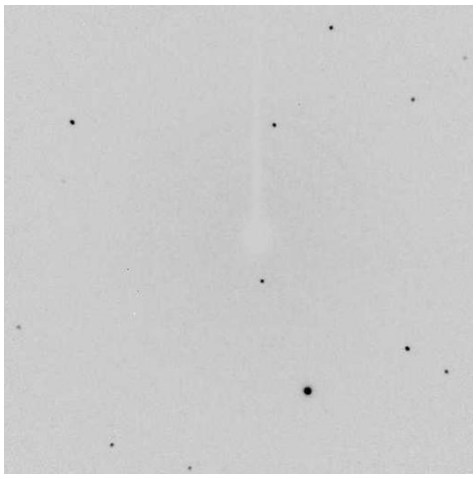

Powder diffraction

The use of a point detector leads to powder diffraction profiles of the sort of the ones below

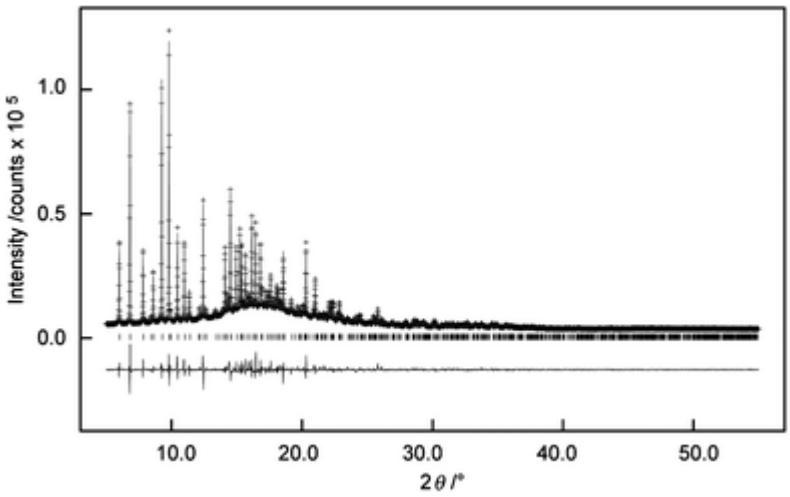

In this case, at each 2ϑ-angle the detector records the diffraction intensity, thus putting forth the classic powder diffraction profile with the Braggs peaks. Each peak is due to the contributions of those reflections whose Bragg angles correspond to the one being explored by the detector.

If one uses a PSD, then diffraction rings are obtained, according to what reported below

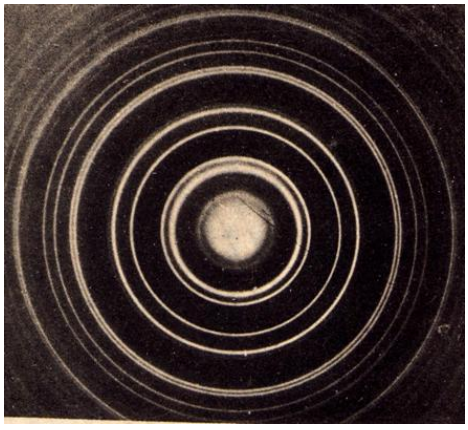

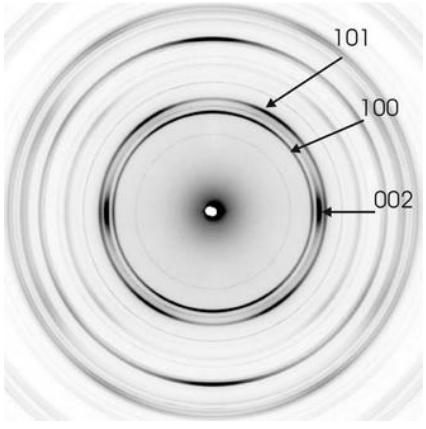

Such diffraction rings can be converted into the conventional *I*-2ϑ profile, by means of appropriate software, to obtain

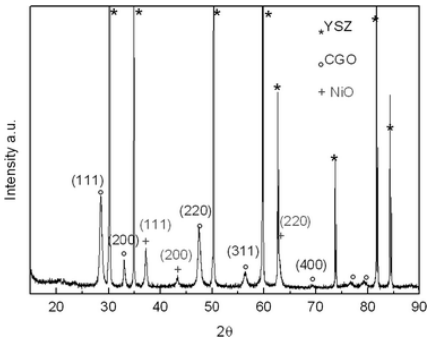

The relationship between experimental geometry and Bragg angle is displayed below

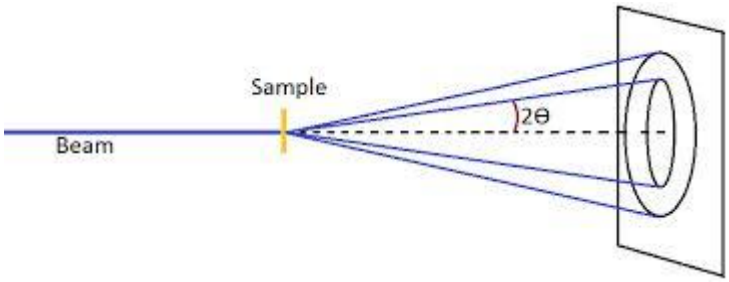

and results in
tg(2ϑ)=*r*/D,
where *r* is the radius of a diffraction ring and D the distance between detector and sample.

INEL inc. produces particular detectors given by an array of PDs, to have an instrumental geometry like the one below

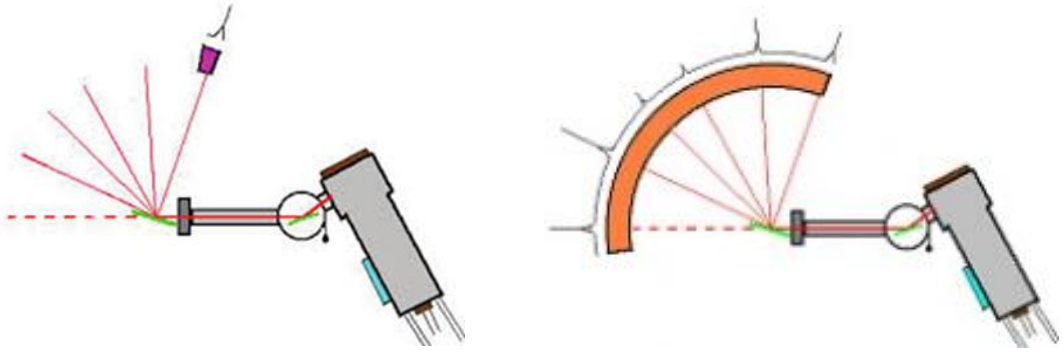

that is implemented through the instrument shown beneath

Detectors' functioning principles

Quantum Detection Efficiency (**QDE**) = ratio of photons absorbed by the detection system over the incident ones.
Dead Time (**DT**) = it is the minimum time between two events so that the detector reveals them as separate.

Scintillation Detectors **(from the internet)**

In the scintillation counter, the conversion of X-ray photons into an electrical signal is a two-stage process. The X-ray photon collides with a phosphor screen, or scintillator, which forms the coating of a thallium-doped sodium iodide crystal. The latter produces photons in the blue region of the visible spectrum. These are subsequently converted to voltage pulses by means of a photomultiplier tube attached directly behind the scintillator. The number of electrons ejected by the photocathode is proportional to the number of visible photons which strike it, which in turn is proportional to the energy of the original X-ray photon. Due to a large number of losses, the energy resolution of the detector is poor, and as such it cannot be used to resolve X-ray photons due to Kα and Kβ radiation. However, it has a very high quantum efficiency and a very low dead time making it the ideal detector for the point intensity measurements required for step-scanning diffractometers.

Gas-filled Detectors **(from the internet)**

The second type of detector commonly used in the laboratory is the gas-filled detector. This detector works on the principle that X-ray photons can ionize inert gas atoms such as argon or xenon into an electron (e^-) and ion (e.g. Ar^+) pair. The ionization energy required to eject an outer electron is low (10-20 eV) compared to the energy of the X-ray photon (8 keV) so that one X-ray photon can produce several hundred ion pairs. A wire placed inside the detector is set to a potential of about 1000 V. This accelerates the electrons of the ion pair towards the wire causing further ionization and an enhanced signal by gas amplification. The burst of electrons on the wire is converted into a voltage pulse which is then shaped and counted by the electronics. In order to minimise the dead time of the system, a quenching gas such as methane (CH_4) is mixed with the inert gas (e.g. 90% Ar : 10% CH_4).

A disadvantage of gas-filled detectors is their loss of linearity at high count rates, but they have a better energy resolution than scintillation detectors. The simple gas-filled detector is much less-commonly used than a more sophisticated form known as a position sensitive detector or PSD.

PSDs are gas-filled detectors with a long poorly-conducting anode wire to which a high tension voltage is applied at both ends. In consequence, the pulse moves towards both ends of the wire simultaneously and by measuring the rate at which it arrives at both ends of the wire, it is possible to determine from whereabouts on the wire the pulse originated. The pulses are stored in a multi-channel analyser (MCA) device according to the pulse position on the wire. This enables PSDs to record data over a whole range of scattering angles, which can be useful where speed of acquisition is crucial, e.g. in time-resolved powder diffraction or thermos-diffractometry. PSDs come in a variety of shapes and sizes: Small PSDs usually have a straight wire and can only collect data over, say, 5-10° 2θ. Large PSDs require curved wires, but collect over a much wider range of scattering angle. In addition, some gas-filled PSDs are sealed, while others require a continuous flow of gas for their operation.

In contrast to the scintillation and simple gas-filled detectors used for point intensity measurements, position sensitive detectors require careful calibration for both wire position and efficiency so that both scattering angles and intensities can be reliably determined. For each channel of the MCA an exact 2θ position is required together with an efficiency coefficient. The wire efficiency can be determined using a sample such as an amorphous iron foil that produces a very high flat background and no Bragg peaks. The 2θ calibration is achieved by scanning the different parts of the detector through the Bragg reflection of a strong peak (or peaks), e.g. the Si 111 peak. For very large curved detectors, the 2θ calibration has to be made using many diffraction peaks.

INEL-like curved detectors **(from the internet)**
Equinox PSD detectors are either a linear or curved chamber into which a solid blade anode and segmented cathode is mounted. Within the chamber there is also a cathode assembly and with the addition of argon / ethane gas, the detector can be defined as a proportional type detector. When an X-ray photon becomes incident on the detector anode an electrical charge develops on the cathode at a position that is spatially coincident with the incident photon. This electrical charge can be measured in terms of its intensity and position about the anode / cathode by way of a delay line. This signal is digitized and then stored in an electronic card. The desired S:N is achieved by multiscan accumulation. In practice, an excellent diffraction pattern can be recorded in just a few seconds and at very high resolution.

Charge Coupling Device (CCD)
It relies on the recording principle illustrated by the pictures below

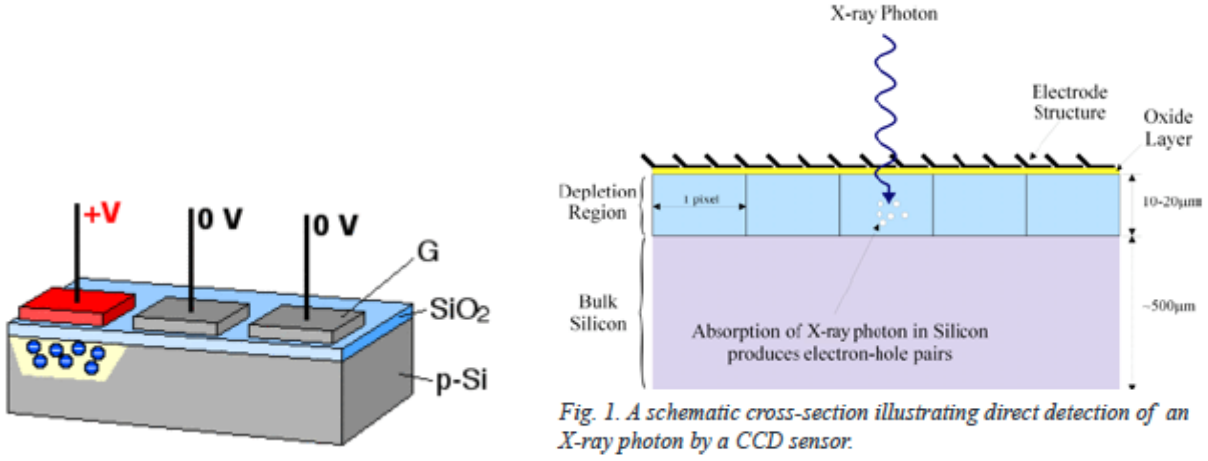

Fig. 1. A schematic cross-section illustrating direct detection of an X-ray photon by a CCD sensor.

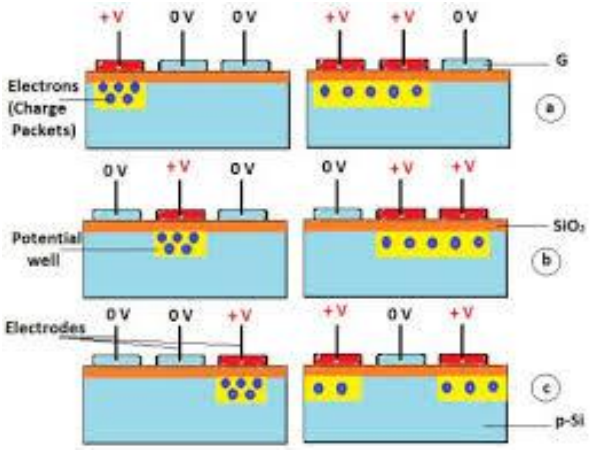

(from the internet)

Leaving aside any claim of precision, the general principle of a CCD-device bases on that one photon generates electron-hole pairs, which are then read by electronics and turned into a digital copy of the light patterns falling on the device. Such a recording technique is possible thanks to photon-sensitive elements called pixels, which form an array receiving the incident radiation. CCDs come in a wide variety of sizes and types and are used in many applications from cell phone cameras to high-end scientific applications.

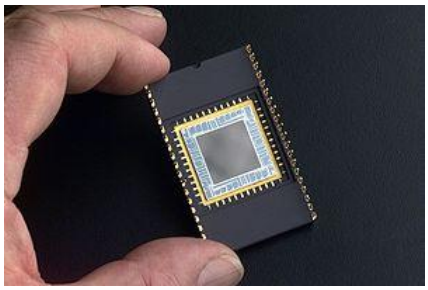

Image plate **(from the internet)**

Imaging Plate (IP) technology has been in existence for many years. Invented and patented in 1975 the flexible storage phosphor IP is similar to a standard x-ray fluorescent screen in physical appearance. It contains a phosphor layer of fine-grained, barium fluoro-halide crystals doped with a divalent europium (Eu^{2+}). When the storage phosphor IP is exposed to x-rays, electrons of the screen are excited to a higher energy level and are trapped in halide vacancies to form color centers. Holes created by the missing valence electrons cause Eu^{2+} to become Eu^{3+}. This latent image is stable for up to several days.

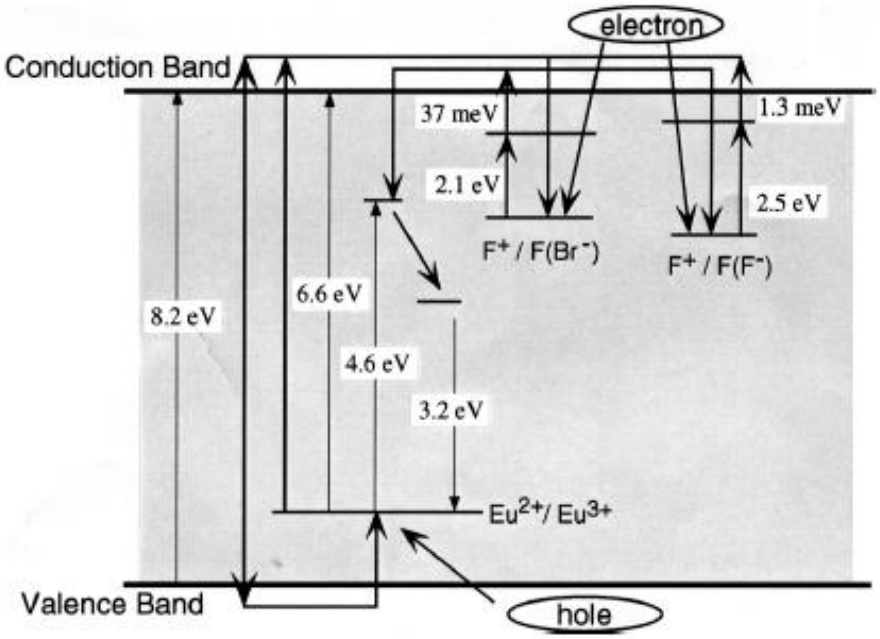

XVIII. EXPERIMENTAL GEOMETRIES

Single Crystal X-ray diffraction geometries

Single crystal X-ray diffraction (SC-XRD) can be operated though two main experimental geometries historically based on *point detectors*, according to which diffractometers are then designed:

1) Four circle geometry (**FCG**; also dubbed ‘’Eulerian Geometry’’);
2) K-geometry (**KG**).

Both aim at allowing the experimenter to orient a crystal in any possible direction, in order to have it in a position appropriate to fulfill the Bragg diffraction conditions. This must be accomplished in such a way that the crystal is kept in the same place upon any rotation (*i.e.* it must have an eucentric position). For such a purpose, the crystal is mounted on a thin glass pole, place successively on a goniometer-head (see below) that provides all adjustments required.

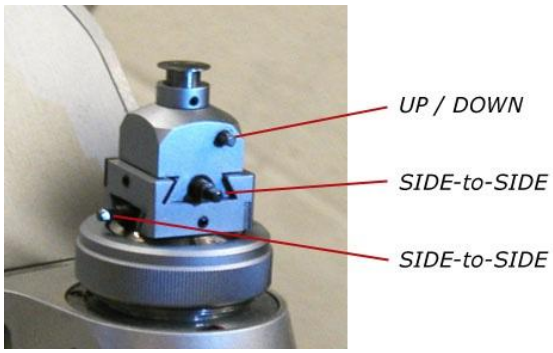

The general principles of designing a **FCG**-diffractometer is shown below

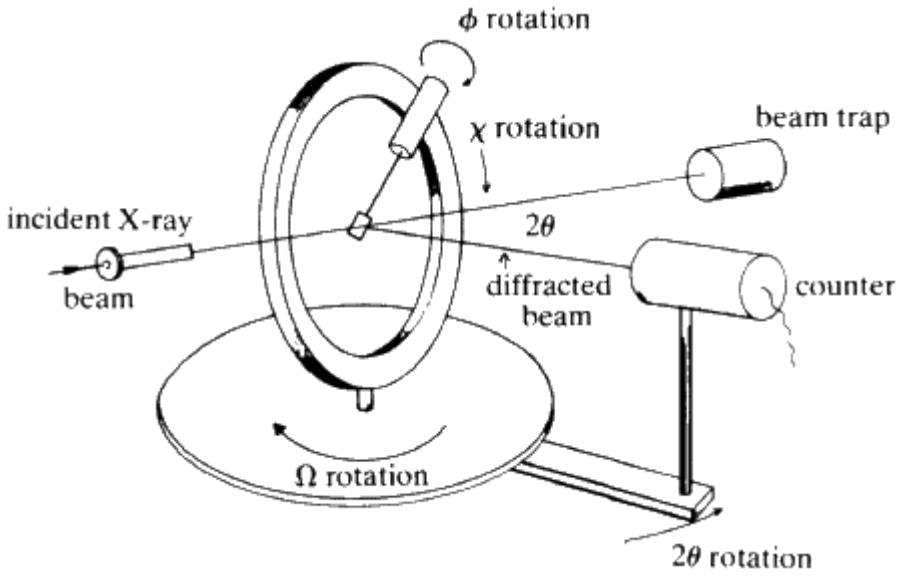

The Ω-χ-ϑ-ϕ axes allow it to orient the crystal in any possible way, so that the same diffraction processes can be measured with more than one crystal orientation.

The pictures below display the arrangement for **KG**.

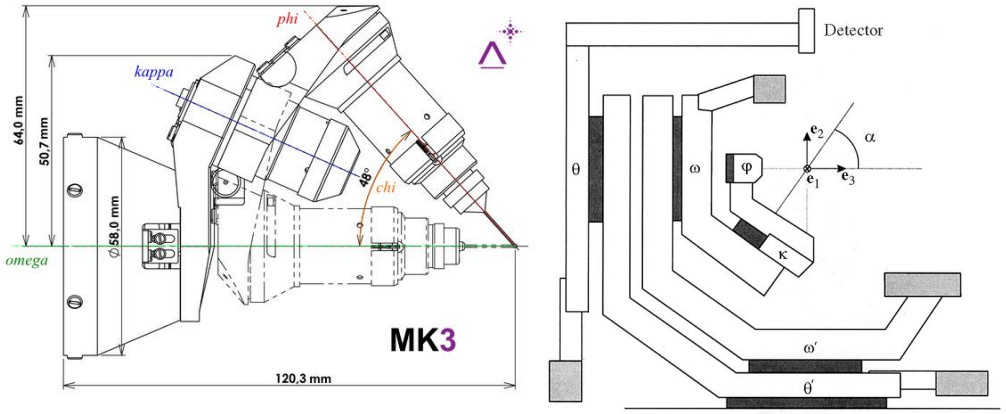

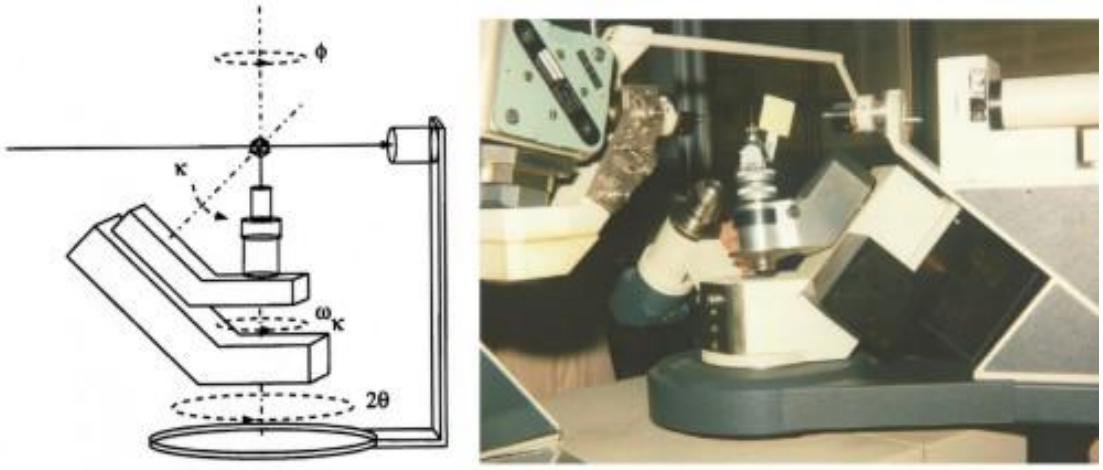

Such geometries allows one to collect *hkl*-intensities using different rotation axes to orient the single crystal under study.

A relevant difference occurs in terms of data collection approach if one uses a Charge-Coupled-Device as a detector. This case is shown in the picture below.

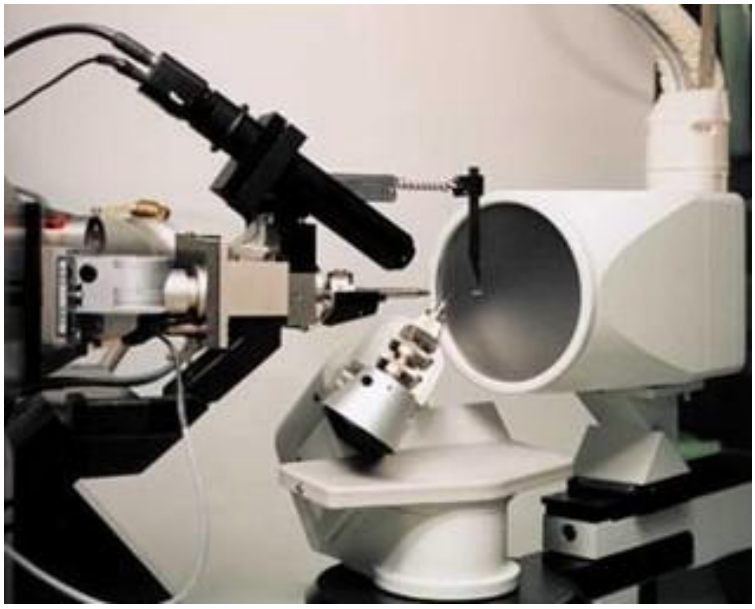

The possibility to record many reflections at a time implies much shorter data collection times. The geometry is a **K**-type.

The recording-architecture leads to specific data-reduction procedures.

X-ray powder diffraction geometries

We distinguish two main experimental geometries to perform X-ray powder diffraction experiments:

1. Bragg-Brentano (**BB**) architecture;
2. Deby-Scherrer (**DS**) setup.

The first one is also known as “parafocusing geometry”. It follows the principle displayed in the Figure below.

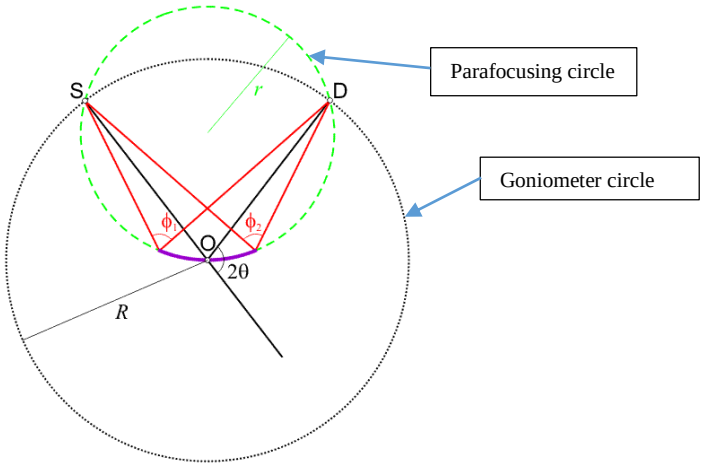

The goniometer circle has a fixed radius, *R*, and depends on the manufacturer. It affects the angular resolution of the diffractometer. The parafocusing circle (or focusing circle) center is placed on the bisector of the SOD angle, and changes as a function of 2θ. The very principle of such a geometry is related to the fact that ϕ, and SOD are equal to each other (180-2θ), and correspond to the same scattering angle 2θ.

The second one is often addressed to as transmission geometry. The principle is to strike a sample, placed for instance in a capillary, with an incident X-ray beam, and collect the diffraction pattern. If one uses a 2D-detector, then the diffraction rings are generated, as already stated. Other possible collection architectures are available, using nowadays multi-strip detectors. In the Figure below the transmission principle is represented.

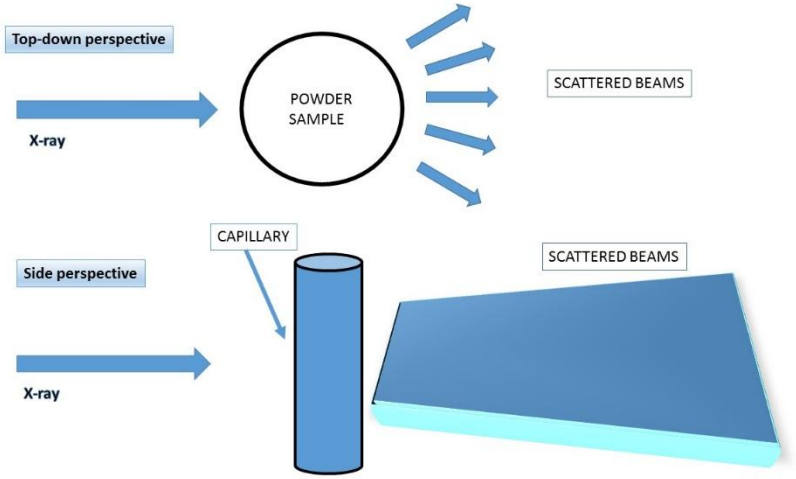

SUGGESTED READINGS (TEXTBOOKS)

Boisen MB and Gibbs GV (1990) Mathematical Crystallography, Reviews in Mineralogy, Vol 15, Mineralogical Society of America
Egami T and Billige SJL (2003) Underneath the Bragg peaks: structural analysis of complex materials, Pergamon Materials Series, Ed. R.W.Cahn
Snyder RL, Fiala J, Bunge HJ (1999) Defect and microstructure analysis by diffraction, Oxford University Press
Woolfson (1970) MM X-ray Crystallography, Cambridge University Press